Comments to reviews of our manuscript, # bg-2018-138

Dear editor,

we appreciate the positive evaluation of our manuscript entitled "A systematic look at chromium isotopes in modern shells – implications for paleo-environmental reconstructions" by two anonymous reviewers. We are thankful for their constructive comments and the suggestions added by associate editor Aninda Mazumdar. We have implemented their suggestions in a revised manuscript and respond in a point-by-point manner below:

Referee #1

We have implemented and corrected the technical corrections pointed out by this reviewer.

1. All units are now separated from the respective numbers
2. Corrected to δ^{53}Cr
3. Corrected to δ^{53}Cr
4. Corrected to Pereira et al. (2015)
5. "1" inserted
6. Excluded "a"

Referee #2

Technical comments: we have now transferred discussion text inter mingled the results chapter to the actual discussion chapter. We now instead discuss the seawater data and data from the respective shell transect in separate short sub-chapters (5.1 and 5.2).

There is a lack of modern seawater – carbonate sediment pair data that would make calculations of distribution coefficients for abiogenic carbonates possible. We have added, at the end of chapter 5.3, a respective distribution coefficient value from the data in Holmden et al. (2016) for seawater and carbonate sediment form Jamaica, to our knowledge the only data set that allows for calculation of an abiogenic distribution coefficient.

To our recollection we intensely discuss all the possibilities for explaining the isotopically light Cr uptake into calcifying organisms in our discussion. We here emphasize that the isotopically light Cr signatures measured in all shells are compatible with results from foraminifera and corrals and all in all point to a redox process during Cr uptake into the shell carbonates. With the presently scarce data sets available, Cr(III) uptake via organic ligands would rather prefer isotopically heavy Cr as suggested by Saad et al. (2017), a contribution which we cite in our manuscript.

Line 371. Added the "."

Line 650: changed to "on average"

Line 750: changed to "future".

Associate editor Aninda Mazumdar

A. We have clarified the requirements for sample sizes in the respective chapter. We do not have TOC values of the sample studied that could substantiate the relation between Cr concentrations and organic material in the shells. Our incineration experiments however clearly point to the importance of organic matter in this respect.

B. We would like to keep the reference to the Farkas et al. paper as our study is a direct follow up on Farkas et al.'s investigations. The Farkas et al. manuscript is now in press with *Earth and Planetary Science Letters*, and it will be potentially published completely at the time our study could be published in *Biogeosciences*. For your convenience, we have uploaded the "proofs" of the Farkas et al. paper soon to appear. The reason why we would like to keep referring to this study is that it is the only one to data that allow a comparison of marine mollusk Cr isotope data with ambient seawater and therefore sets an appropriate frame for our contribution. We allows us to amend (following the our own marked up revised manuscript) the proofs of the Farkas et al paper as a guarantee/proof that this article is now officially in press and soon to be allocated respective volume, issue and page numbers.

C. We fully agree that the Ce anomaly – Cr isotope relationship in Farkas et al. has no relationship to our study, and we have therefore deleted all the parts that refer to this peculiarity in our revised manuscript.

D. It is correct that we do not have Eh and oxygen data on the surface waters in which the mollusks thrived. In this respect, we do not have control on seasonal variations in Cr concentrations and Cr isotopes that could substantiate the intra-species variations we see in the transect samples. All we can say at his stage is that we have results that show redox variations in surface waters recorded in Baltic seawater (study by Paulukat et al. 2015, cited in our manuscript), which clearly are dictated by algae blooms that fractionate and strip Cr effectively form the water columns.

E. We would strongly disagree with this as hitherto no solid experimental data exist that constrains isotope effects during inorganic incorporation of Cr into carbonates. The only study that approaches this issue is that by Rodler et al. which we extensively cite in our manuscript.

F. We have tried to shorten the manuscript as much as possible, particularly we have deleted sections in the chapter that describes our model in relation to known observations of organic material in shell structures. Also, the many referring paragraphs to Farkas et al. with respect to Ce anomalies are deleted. However, we would like to keep the aspects of paleo redox reconstructions that potentially are doable when appropriate data on modern systems are available. The major aim with using shells as marine Cr isotope archives is their potential use for reconstructing redox variations in ancient oceans, with important implications and links to climate change on land.

We hope that our revised manuscript is a significantly improved version that meets the standards of Biogeosciences for publication.

Thanks in advance and very best regards

Robert Frei (on behalf of all coauthors)

A systematic look at chromium isotopes in modern shells – implications for paleo-environmental reconstructions

Robert Frei[1*], Cora Paulukat[1,2], Sylvie Bruggmann[1], Robert M. Klaebe[1]

[1] Department of Geoscience and Natural Resource Management, University of Copenhagen, Øster Voldgade 10, 1350 Copenhagen K, Denmark

[2] ALS Scandinavia AB, Aurorum 10, 977 75 Luleå, Sweden

* Correspondence to: Robert Frei (robertf@ign.ku.dk)

Abstract. The chromium isotope system ($^{53}Cr/^{52}Cr$ expressed as $\delta^{53}Cr$ relative to NIST SRM 979) in marine biogenic and non-biogenic carbonates is currently being evaluated as a proxy for the redox state of the ocean. Previous work has concentrated on using corals and foraminifera for this purpose, but investigations focusing on the behavior of Cr in bivalves as potential archives are lacking. Due to their often good preservation, fossil marine biogenic carbonates have the potential to serve as useful archives for the reconstruction of past ocean redox fluctuations and eventually link those to climatic changes throughout Earth's history. Here, we present an evaluation of the Cr isotope system in shells of some modern bivalves. Shell species from Lucidinadae, Cardiidae, Glycimerididae, and Pectenidae, collected systematically from one Mediterranean location (Playa Poniente, Benidorm, Spain) over a three year period, reveal $\delta^{53}Cr$ values ranging from 0.15 to 0.65 ‰, values that are systematically below the local seawater $\delta^{53}Cr$ value of 0.83 +/- 0.05 ‰. This attests for significant reduction of dissolved seawater chromium in the process leading to calcification and thus for control of Cr isotope fractionation during biological routes. A similar, constant offset in $\delta^{53}Cr$ values relative to surface seawater is observed in shells from *Mytilius edulis* from an arctic location (Godhavn, Disko Bay, Greenland). Chromium concentrations in the studied shells are significantly controlled by organic matter and typically range from 0.020 to 0.100 ppm, with some higher concentrations of up to 0.163 ppm recorded in Pectenidae. We also observe subtle, species-dependent differences in average Cr

1

isotope signatures in the samples from Playa Poniente, particularly of Lucidinadae and Cardiidae, with considerably depressed and elevated δ^{53}Cr values, respectively, relative to the other species investigated. Within-species heterogeneities, both in Cr concentrations and δ^{53}Cr values, are favorably seen to result from vital effects during shell calcification rather than from heterogeneous seawater

30   composition. This is because we observe that the surface seawater composition in the particular Playa Poniente location remained constant during July month of the three years we collected bivalve samples. Within single shell heterogeneities associated with growth zones reflecting one to several years of growth, both in δ^{53}Cr and Cr concentrations, are observed in a sample of *Placuna placenta* and *Mimachlamys townsendi*. We suspect that these variations are, at least partially, related to

35   seasonal changes in δ^{53}Cr of surface seawaters. Recognizing the importance of organic substances in the bivalve shells, we propose a model whereby reduction of Cr(VI) originally contained in the seawater as chromate ion and transported to the calcifying space, to Cr(III), is effectively adsorbed onto organic macromolecules which eventually get included in the growing shell carbonates. This study, with its definition of statistically sound offsets in δ^{53}Cr values of certain bivalve species from

40   ambient seawater, forms a base for futures investigations aimed at using fossil shells as archives for the reconstruction of paleo-seawater redox fluctuations.

1. Introduction

Redox processes on land lead to mobilization of Cr from weathering rocks and soils into the run-off. It is now known that oxidation of silicate- and oxide mineral hosted Cr(III), potentially with

45   catalytic help of MnO_2, to Cr(VI) is accompanied by an isotopic fractionation rendering the mobilized Cr(VI) isotopically heavier (Ellis et al., 2002;Zink et al., 2010;Døssing et al., 2011) . Recently, an alternative, redox-independent pathway of Cr mobilization, through ligand-promoted dissolution of Cr-containing solids, was advocated by Saad et al. (2017). This mobilization path bases on the ability of organic acids and siderophores to efficiently bind Cr(III) whereby respective ligand formation is

2

50   accompanied by isotope fractionation effects, leading to Cr(III) being enriched in ^{53}Cr very much like in redox-dependent mobilization paths.

The fate of Cr transported to the oceans, its transfer/removal to marine sediments and its cycling through marine organisms, is largely unexplored and complex. Much research focus today is on the understanding of the redox cycling of Cr in the ocean system, and on investigating marine

55   sediments and marine organisms as potential archives for recording past redox conditions of the ocean-atmosphere system through geological time (Frei et al., 2009;Frei et al., 2011;Frei et al., 2013;Frei et al., 2016;Bonnand et al., 2013;Planavsky et al., 2014;Holmden et al., 2016;D'Arcy et al., 2017;Rodler et al., 2016a;Rodler et al., 2016b;Gilleaudeau et al., 2016). It is conceivable that the Cr isotope composition of seawater and marine chemical sediments reflect a complex signal of

60   oxidation/reduction processes operating within the oceans (Scheiderich et al., 2015;Paulukat et al., 2016), and it is therefore that one must first understand the individual processes and mechanisms that governs the transfer of dissolved Cr in seawater into the respective potential archives. Recent studies (Rodler et al., 2015;Pereira et al., 2015;Wang et al., 2016) have paved the road, but further systematic investigations in both natural and laboratory-controlled settings are required.

65   ~~Although naturally depleted in chromium (containing only ppb to ppm levels), marine carbonates provide a potentially valuable archive of (i) the paleo-seawater δ^{53}Cr composition, and/or (ii) the past redox conditions of the oceanic water masses. Due to basically continuous geological record of marine carbonates throughout most of the Earth's history, the Cr isotope studies on marine carbonate archives are appealing and potentially relevant to addressing the bigger question of the~~

70   ~~Earth's oxygenation and temporal evolution of atmospheric O$_2$ levels through geological time. Nevertheless, as shown by recent studies (Rodler et al., 2015;Pereira et al., 2015;Wang et al., 2016) the actual mechanism(s) of the redox-controlled isotope fractionation associated with the incorporation of Cr from seawater into inorganic and biogenic carbonates is rather complex and poorly understood, thus requiring further systematic investigations in both natural and laboratory-controlled~~

75   ~~settings.~~

Available results from inorganic calcite precipitation experiments revealed that the incorporation of Cr from a solution into $CaCO_3$ is facilitated as chromate anion (CrO_4^{2-}), which replaces carbonate anion (CO_3^{2-}) in the calcite lattice (Tang et al., 2007). This process of inorganic calcification tends to preferentially incorporate heavy [53]Cr isotopes into the mineral, yielding the $\delta^{53}Cr$ of calcite that is up to ~0.3 ‰ more positive compared to the fluid; unless the latter is a Cr-poor solution (such as seawater) in which case the isotope fractionation between inorganic calcite and the fluid is negligible (Rodler et al., 2015).

In contrast, results from biologically produced $CaCO_3$ minerals, such as foraminiferal calcite (Wang et al., 2016) and/or coral aragonite (Pereira et al., 2015), confirmed that these marine organisms produce $CaCO_3$ skeletons that are systematically negatively fractionated , up to ~1 ‰, compared to ambient seawater. Similarly, data by Holmden et al. (2016) from the modern Caribbean Sea show that the $\delta^{53}Cr$ of bulk carbonate sediments is about 0.46 ± 0.14‰ lower relative to local seawater. These results therefore oppose those from inorganic calcite precipitation experiments (cf., Rodler et al. (2015)).

Furthermore, due to a local redox cycling and biological uptake of Cr in the oceans (Semeniuk et al., 2016), the Cr isotope signature of present-day seawater is not globally homogeneous (Scheiderich et al., 2015;Paulukat et al., 2016). This additionally complicates the application of $\delta^{53}Cr$ measurements in marine carbonate archives with respect to deducing information regarding global ocean redox, and implications thereof for climatic changes, on Earth through time. Considering the abovementioned issues and limitations, the full potential of Cr isotopes for paleo-redox studies can only be realized with more detailed calibration work done on modern *seawater-carbonate systems* from different oceanographic settings and locations, where $\delta^{53}Cr$ data can be collected simultaneously from (i) local ocean waters, and (ii) precipitated inorganic/biogenic carbonates.

This contribution is a follow-up of a recent study by Farkaš et al. (in press) who for the first time present a comprehensive Cr isotope investigation of a coupled *seawater-carbonate system* from one of the world's largest carbonate-producing shelf ecosystems, the Great Barrier Reef (Lady Elliot

Island, Australia). These authors present δ^{53}Cr data from local seawaters and selected recent biogenic carbonates (i.e., gastropods, cephalopods, corals, and calcifying algae), complemented by additional δ^{53}Cr analyses of marine skeletal carbonates (i.e., bivalves, gastropods, and cephalopods) collected from main oceanic water bodies including North and South Atlantic Oceans, North and South Pacific Oceans, and the Mediterranean Sea. ~~A tight coupling between δ^{53}Cr values and cerium anomaly (Ce/Ce*) data from the marine skeletal carbonates led these authors to conclude that marine biogenic carbonates that precipitated from seawater and/or calcifying fluid under the most oxic conditions (i.e., having the most negative Ce/Ce*) can actually reflect the Cr isotope signature of ambient ocean water, shown by a sample of microbial carbonate (i.e., coralline red algae) collected at Lady Elliot Island~~. Our study goes a step further in that we compare Cr isotope signatures of certain bivalve species from one location in the Mediterranean Sea collected over a period of 3 years with simultaneous collection of surface seawater from that location. This allows us to elaborate on inter-and intra-species Cr isotope variations, with the ultimate aim to eventually deduce systematic fractionation trends/offsets relative to ambient seawater compositions, that could later be used for reconstructing the redox state of past ocean waters.

2. Study sites and samples

Bivalve shells (from families Cardiidae, Veneridae, Glycymerididae, Pectinidae, and Lucinidae) and ambient surface seawater samples were collected during the first two July weeks in three successive years from 2015-2017, at Mediterranean Playa Poniente beach, Benidorm, Spain (N38°32'4.20" W0°8'57.30"; Fig.1). In addition, *in situ* growing alive *Mytilus edulis* species and seawater samples were collected by researchers from the Center for Permafrost (CenPerm), University of Copenhagen, at a rocky coast section near arctic Godhavn (Qeqertarsuaq), Disko Island, Greenland (N69°14'44.14" W53°31'38.34"; Fig.1) during fieldwork in June 2016. Respective seawater analyses from the same locations, except the 2017 Playa Poniente sample, were performed earlier and published in Paulukat

5

et al. (2016). Two additional bivalve shells (*Placuna Placenta*; *Mimachlamys townsendi*) from Kakinada Bay, Andhra Pradesh, India (N16°55'30.85" E82°15'43.36"; Fig. 1) and from Hawke's Bay Beach,

130   Karachi, Pakistan (N24°51'36.46" E66°51'36.66"; Fig. 1), respectively, were used to investigate intra-shell Cr isotope - and Cr concentration ([Cr]) variations. These specimen were cut along a growth transect into sub-samples and analyzed individually. Pictures of representative shell species (with the sub-sample growth transects of the two specimen studied for intra-shell variations) studied herein are depicted in Figure 2.

135   Bivalve species studied from Playa Poniente all live in sand in an intertidal setting to about 20 m depth. While exact ages of the species studied are not known, based on the relatively small sizes and number of annual growth zones in Glycymeris (Beaver et al., 2017;Yamaoka et al., 2016) and *Callista chione* (Moura et al., 2009) we estimate the age range of the majority of shells sampled between ~2-5 years. *Mytilus edulis* lives in the intertidal and sublittoral (up to 5m depth) on a wide

140   range of habitats from rocky shores to estuaries. Our samples were collected from a rocky coast intertidal environment near Godhavn. Growth rates in *Mytilus edulis* are highly variable and dependent on location and environmental conditions. Typically, under optimal conditions, *Mytilus edulis* can grow up to 60-80 mm in length within 2 years (Seed and Suchanek, 1992). *Placuna placenta* (window pane oyster, Capiz) species from Kakinada Bay were purchased from a fisherman who hand-

145   picked them at low tide in a water depth of ~1 m. Windowpane oysters from this location have been reported to attain an average length of 122 mm in 1 year and 157 mm in 2 years (Murthy et al., 1979). The *Placuna placenta* sample studied herein, measuring ~10 cm from the apex to the rim (Fig.2), therefore represents about a one year growth period. The Pectenidae species, determined as *Mimachlamys townsendi*, from Hawke's Bay was collected on the sandy beach in 1969 by the lead

150   author himself. There is an extensive variation in growth rates and attained ages of Pectinidae. Commonly, Mimachlamys has a life time of up to 6 years and in this time reaches sizes between 6-10 cm. Our specimen of *Mimachlamys townsendi* with ~8 cm in length therefore represents a fully grown-up shell and our transect (Fig. 2) is representative of several years of growth. These scallops live

6

usually intertidally in shallow water of up to 10 m depth. Some biological and ecological characteristics

155 of scallops can be found in Minchin (2003).

3. Analytical details

3.1 Sample preparation and dissolution

160

Seawater samples were collected into pre-cleaned plastic bottles, filtered through 0.45 μm nylon membrane filters using a vacuum pump and then acidified and spiked with a ^{50}Cr-^{54}Cr double spike within 1 week from collection.

In order to recover enough Cr for isotopic analyses (>50 ng Cr are usually required for a precise

165 mass spectrometrical analysis), sShell samples (single shell pieces, transect pieces) weighing between 1.5-3 g were required. In cases where individual shell specimen weighed less than this amount, multiple ; up to 7 combined individual shells in case of *Chamelea striatula* and *Loripes lucinalis*) shells from the same species (up to 7 individual shells in case of *Chamelea striatula* and *Loripes lucinalis*) were combined. Samples were first physically brushed and washed in Milli-Q™ water (MQ, resistivity

170 18 MΩ), and then immersed in 2% hydrogen peroxide (H_2O_2) for 10 minutes. They were briefly leached in 0.5N HCl and finally thoroughly washed in MQ water. Ten *Mytilus edulis* shells (five dorsal and 5 ventral shells) were combined and powdered in an agate mortar to be used as a so-called "mixed" sample. With the exception of the *Mytilus edulis* samples from Godhavn which were dissolved directly in *aqua regia* after removal of the mussel tissue, pre-cleaned shells (also including 3 samples of

175 *Mytilus edulis* for comparative purposes) were weighed- into chemical porcelain crucibles (CoorsTek™, 15ml capacity) and ashed in a furnace at 750°C for 5 hours prior to dissolution in 6N HCl. The aim with this incineration was to achieve a total dissolution of the respective shells, including the organic material known to have chromium associated with.

7

3.2 Ion chromatographic separation of chromium~~Chromium isotope analysis (δ⁵²Cr) by TIMS~~

Methods used in this study for the purification and isotope analysis of Cr in seawater samples and biogenic carbonates follow those described in Paulukat et al. (2016) and Pereira et al. (2015), with small modifications. Briefly, filtered and spiked seawater samples were transferred into 1 liter Savillex™ teflon beakers, evaporated, re-dissolved in 50ml of *aqua regia*, and evaporated again. Respective spiking (aiming at a $^{50}Cr/^{52}Cr$ ratio in the sample-spike mixture of between 0.15 to 0.75) of biogenic carbonates was done during the attack with *aqua regia* or during the 6N HCl attack of incinerated samples. Spiking prior to ion chromatographic separation procedures enables correction of any mass-depended Cr isotope fractionation effects that could occur during the chemical purification and/or mass spectrometric analysis of the samples. The acid-digested and dried down samples (i.e., filtered seawaters and pre-cleaned carbonates) were then processed through a two-step Cr purification chromatography, using a combination of anionic and cationic exchange columns. The first step used a pass over columns (Spex™) loaded with 2 ml anion exchange resin. The spiked and dried samples were re-dissolved in ca. 40 ml of 0.1N HCl together with 0.5 ml of a freshly prepared 1N ammonium persulfate ((NH_4)$_2S_2O_8$; Sigma-Aldrich, BioXtra, ≥98%, lot#MKBR5789V)) solution, which acts as an oxidizing agent. The sample solutions, contained in 60 ml Savillex™ teflon vials, were placed in a microwave oven and heated with closed lids for 50 minutes using a low energy thawing program to ensure full oxidation of Cr(III) to Cr(IV). After the samples cooled to room temperature, they were passed through anion exchange columns loaded with 2 ml of pre-cleaned Dowex AG 1 × 8 anion resin (100-200 mesh). The matrix was washed out with 10 ml of 0.2N HCl, then with 2 ml of 2N HCl and finally with 5 ml of MQ H_2O, before Cr was collected through reduction with 6 ml 2N HNO_3 doped with a few drops of 5% H_2O_2. The so-stripped Cr bearing solution was then dried down at 130°C.

The second step used a pass over columns (BioRad™ Econo) loaded with cation exchange resin. For this, the Cr-bearing samples from the anion columns were re-dissolved in 100 µl of concentrated HCl and diluted with 2.3 ml ultrapure MilliQ water. This solution was added to the extraction columns

loaded with 2 ml of pre-cleaned Dowex AG50W-X8 cation resin (200-400 mesh). The extraction procedure principally adhered to that published by Bonnand et al. (2011) and Trinquier et al. (2008) with only small modifications. The final Cr-bearing liquid cut was dried down at 130°C, ready to be loaded for Cr isotopic analysis on the thermal ionization mass spectrometer.

210   Total procedure Cr blanks, including incineration, dissolution, and ion chromatography procedures remained below 4 ng Cr. In the worst case scenario, using the sample with the lowest [Cr] in our study (sample Pec-B; [Cr] = 0.021, sample weight = 2.8 g), such blank contribution (assuming the blank Cr composition is of an igneous Earth inventory one), would induce a change in the $\delta^{53}Cr$ signature of 0.04 ‰. This is below our current level of analytical precision achieved on the samples

215   studied herein, and below the external reproducibility of between +/- 0.05 to 0.08 ‰ for double-spiked NIST SRM 979 (see below) under similar measuring conditions. We therefore did not perform a blank correction of our measured sample Cr isotope signatures.

3.3 Mass spectrometric analyses of Cr

220

The Cr isotope measurements were performed on an IsotopX Ltd. PHOENIX thermal ionization mass spectrometer (TIMS) equipped with eight Faraday collectors that allow simultaneous collection of the four chromium beams (50Cr+, 52Cr+, 53Cr+, 54Cr+) together with interfering 49Ti+, 51V+, and 56Fe+ masses.

225   The separated Cr residues were loaded onto outgassed Re-filaments using a loading solution consisting of 1 µl of 0.5N H_3PO_4, 2.5 µl silicic acid (Gerstenberger and Haase, 1997), and 0.5 µl of 0.5N H_3BO_3. The samples were analyzed at temperatures between 1050-1250°C and 52Cr beam intensities of between 0.35 and 1V. One run consisted of 120 cycles and where possible, every sample was run at least twice. The final $\delta^{53}Cr$ values of the samples were determined as the average of the repeated

230   analysis and are reported in per mil (‰) with ± standard deviation (2σ) relative to the international standard reference material NIST SRM 979 as:

$$\delta^{53}Cr\ (‰) = [(^{53}Cr/^{52}Cr)_{SAMPLE} / (^{53}Cr/^{52}Cr)_{NIST\ SRM979} - 1] \times 1000$$

235   The within-run two standard errors of the measurements reported in this study were consistently ≤ 0.1‰. The external reproducibility was determined using average $\delta^{53}Cr$ values of double spiked NIST SRM 979 measured under the same conditions as the samples on the Phoenix. Figure 3 depicts the averages of 10 runs each from the same filament loaded with 200 ng of double spiked NIST SRM 979 at beam intensities of 0.35V and of 1V. The external reproducibility of the standard under

240   these conditions was +/- 0.08‰ and 0.05‰ (2σ), respectively, at the above mentioned ^{53}Cr beam intensities (Fig. 3). The average composition of the 0.35V and 1V multiple NIST SRM 979 runs analyzed during the course of this study shows an average offset of +0.04 ± 0.03‰ (2σ; n=11; Fig. 3) on our machine compared to the 0‰ certified value of this standards. This offset stems from the original calibration of our double spike relative to the NIST 3112a Cr standard, and the observed offset of

245   0.04‰ was deducted from the raw $\delta^{53}Cr$ results to account for this small discrepancy.

4. Results

4.1. Surface seawater - Chromium isotope compositions ~~(δ⁵³Cr)~~ and ~~elemental~~ chromium concentrations

250

Table 1 lists the Cr isotope compositions and Cr concentrations the of surface seawater samples relevant to this study. Waters collected during 4 subsequent years in July from Playa Poniente yield surprisingly homogeneous Cr isotope compositions and dissolved [Cr] that range from $\delta^{53}Cr$ = 0.81 – 0.85‰, and from 222 – 280 ng/kg, respectively. These are comparable with surface seawater

255   data ($\delta^{53}Cr$ = 0.81 – 0.96‰, [Cr] = 239-306 ng/kg) collected from Playa Albir, a beach situated ca. 9.5 km to the ENE of Playa Poniente (Fig. 1), in the years 2013 through 2015 (data published by Paulukat et al. (2016)). ~~The Playa Poniente data are compatible with data from other Mediterranean surface~~

10

4.2 Shells - Chromium isotope compositions (δ⁵³Cr) and chromium concentrations

265

Cr isotope compositions and [Cr] of a variety of bivalve species from Playa Poniente (an

undefined species of Cardiidae, *Callista chione*, *Chamelea gallina*, *Chamelea striulata*, an undefined

species of Glycymeris, *Loripes lucinalis*, *Pecten jacobaeus*, *Venus verrucosa*, *Venus nux*, and *Arca

270 Navicularis*), of *Mytilus edulis* species from Godhavn, and of sub-samples from a window pane oyster

(*Placuna placenta*) from Kakinada Bay and of a specimen of *Mimachlamys townsendi* (Pectenidae)

from Hawke's Bay Beach are listed in Table 2. Respective data are plotted in Figs. 4-7, together with

the ranges of local surface seawaters and the range of igneous Earth reservoirs as defined by

Schoenberg et al. (2008). There is no obvious correlation between δ^{53}Cr and [Cr] data (r^2= 0.18),

275 diagram not shown) of the samples analyzed herein.

Bivalves collected from Playa Poniente generally show low and scattered Cr concentrations

ranging from 0.027 to 0.163 ppm, with the largest variations recorded in Glycymeris, and the

systematically highest concentrations measured in species of *Pecten jacobaeus* (Fig. 4; Table 2).

Isotopically, the assembly of shell data from Playa Poniente point to a rather restricted compositional

280 band with δ^{53}Cr data ranging from 0.157 to 0.636 ‰, significantly lower than the local surface

seawater average over four consecutive years of δ^{53}Cr = 0.83 +/- 0.05 ‰ (Fig. 4). On closer inspection,

we however note some distinctive Cr isotope ranges defined by the different bivalve species analyzed.

So, for example, samples from Cardiidae exhibit the highest (δ^{53}Cr = 0.60+/-0.13 ‰) -, while samples

from *Loripes lucinalis* show the lowest Cr isotope compositions (δ^{53}Cr = 0.21 +/- 0.10 ‰; Table 2, Fig.

4). One subsample of *Loripes lucinalis* (sample PP 15 D unashed; Table 2) was dissolved in *aqua regia* without prior incineration. This specific sample yielded a distinctively lower Cr concentration ([Cr] = 0.027 ppm) compared to all other *Loripes lucinalis* samples, but at the same time a δ^{53}Cr value which statistically cannot be distinguished from the other *Loripes lucinalis* samples (Fig. 4). While this, as expected, points to the fact that a significant fraction (in fact roughly 50% in case of *Loripes lucinalis)* of the total Cr budget in biogenic carbonates is associated with organic material, and not with carbonate itself, it also points to the likelihood that there is not much difference in the Cr isotope composition of these two potential Cr host materials. This result is substantiated and supported by our study of *Mytilus edulis* from artic Godhavn (see below). Last not but least, we do not see any statistically significant and systematic differences in Cr isotope compositions and Cr concentrations between bivalve species collected during the consecutive sampling years. This conforms to the rather homogeneous surface seawater compositions analyzed from Playa Poniente and the neighboring location Playa Albir during the entire sampling period (Table 1).

Results of entirely *aqua regia* dissolved half-shells of *Mytilus edulis* from Godhavn in the Disko Bay, Greenland, are plotted in a similar combined δ^{53}Cr – [Cr] diagram as the shells from Mediterranean Playa Poniente in Figure 5. These analyses are complemented by a bulk analysis of powdered multiple *Mytilus edulis* specimen from the same location. In addition, two specimen (in each case the dorsal or ventral shell counterparts of the respective *Mytilus edulis* specimen dissolved by *aqua regia*; i.e. samples God-4 and God-5; Table 2) were ashed before final dissolution, in order to evaluate the importance of Cr associated with organic material in these shells compared to the total Cr budget. This was also done with an aliquot of the powdered *Mytilus edulis* mix. All data define an average δ^{53}Cr value of 0.11 +/- 0.05 ‰ (n=10; 2σ), significantly lower than the local surface seawater of 0.73 +/- 0.05 ‰ (Paulukat et al. (2016); Fig. 5). [Cr] for *aqua regia* dissolved specimen are a bit more variable, defining an average of [Cr] = 0.039 +/- 0.009 ppm (n=7, 2σ). Again, the incinerated aliquots,

12

while isotopically not distinguishable from the unashed samples, yielded about twice as high a [Cr] ([Cr] = 0.068 +/- 0.004 ppm (n=3, 2σ)). As mentioned above, this indicates that organic material, effectively attacked by incineration, is a major and significant host of Cr in these bivalves, besides the biogenic carbonate. Again, as already emphasized by the results of *Loripes lucinalis* from Playa Poniente, the two Cr host materials seem not to be isotopically distinguishable. While, with the exception of *Loripes lucinalis*, the negative offset (Δ_{Cr}) of different bivalve species from local surface seawater at Playa Poniente is between ~0.4 to ~0.2 ‰, the respective Δ_{Cr} value for *Mytilus edulis* from Godhavn is higher, ~0.7‰, and comparable to Δ_{Cr} ~0.6‰ defined by *Loripes lucinalis* from Playa Poniente (see details below).

Results from two profiles along respective major growth transects of a specimen of *Placuna placenta* from Kakinada Bay, Andhra Pradesh, India, and a species of Pectinidae (*Mimachlamys townsendi*) from Hawke's Bay, Karachi, Pakistan, are plotted in Figure 6 (*Placuna placenta*) and Figure 7 (*Mimachlamys townsendi*).

[Cr] along the *Placuna placenta* growth profile vary from 0.03 to 0.25 ppm, but this variation is much smaller if the first sample (Cap-A) is excluded. Sample Cap-A incorporates the beak of the shell and a first growth zone which is visually characterized by a more brown (organic-rich) color (Fig. 3). ~~We here attribute the exceptionally high Cr concentration in this sample to increased, organic-rich components which seem to act as efficient Cr hosts, basically reflecting our experiments on *Mytilus edulis* from Godhavn (Fig. 5). Although some fluctuations in [Cr] and δ^{53}Cr values beyond the statistical errors across the beak-margin profile of the studied *Placuna placenta* specimen exist (which we may attribute to local (seasonal?) changes in seawater composition during growth and/or to changing reductive efficiencies during the calcification process), the studied specimen pretty much averages such environmental and biogenic changes out over its entire growth period estimated to be about 2 years. Chromium concentrations in this oyster from the Indian Ocean are comparable with those of the Mediterranean shells studied from Playa Poniente (Table 2, Fig. 4). In contrast, δ^{53}Cr values of *Placuna placenta* are lower than those recorded in the Mediterranean bivalves and show values that are~~

Formatted: Font: Symbol

Formatted: Superscript

13

Intra-species variations of δ^{53}Cr and [Cr] of *Mimachlamys townsendi* from Hawke's Bay are depicted in Figure 7. The average δ^{53}Cr value of all 8 profile samples is 0.07+/-0.11 ‰ (2σ) and statistically indistinguishable from that of *Placuna placenta* (average δ^{53}Cr = 0.05 +/- 0.19 ‰, n= 7, 2σ). With the exception, like in *Placuna placenta*, of the sample closest to the apex/hinge of the shell (sample Pec-H; Fig. 7)) which yielded by far the highest [Cr] in the profile, the [Cr] of the remaining profile samples are ~0.04 ppm. In the specimen studied, the δ^{53}Cr values along the profile are statistically indistinguishable from each other. ~~If Hawke's Bay surface seawater has a δ^{53}Cr similar to that of the Bengal Bay (Paulukat et al., (2015); and assuming it has remained about the same since the collection of the *Mimachlamys townsendi* sample), then *Mimachlamys townsendi* exhibits the same Δ_{Cr} value (~0.5 ‰) as *Placuna placenta* from Kakinada Bay. If calcification processes in *Mimachlamys townsendi* remained constant in terms of biogenic reduction of Cr(VI) to isotopically lighter Cr(III) over the several years of growth of the specimen studied, then this would signify are more or less constant δ^{53}Cr of surface water in this location.~~

5. Discussion

~~The Playa Poniente data are compatible with data from other Mediterranean surface seawaters, which distinguish in [Cr] vs. δ^{53}Cr space from Baltic Sea seawater, but are compatible with the trend of an inverse logarithmic relationship between δ^{53}Cr and [Cr] defined by Scheiderich et al. (2015) and~~

14

substantiated later by Paulukat et al. (2016) of worldwide Atlantic and Pacific ocean waters. Three separate analyses of seawater from Disko Island, published by Paulukat et al. (2016), are characterized by slightly lower [Cr] and δ^{53}Cr values compared to the Mediterranean waters, but are similar to other

365   waters from the North Atlantic (c.f., Fig. 2 in Paulukat et al. (2016)).(2015)

5.11 Present state of knowledge of the behavior of chromium in the marine biogenic carbonate system

370   Chromium-isotope compositions of recent and ancient skeletal and non-skeletal carbonates are currently explored as a (paleo-) redox-proxy for shallow seawater (corals: Pereira et al.(2015); foraminifera: Wang et al.(2016); calcifying algae, molluskes, corals: Farkaš et al. (in press)). The idea behind this approach is that biogenic and non-biogenic carbonates could potentially be used as archives recording the Cr-isotope composition of seawater in which they formed, and with this

375   contribute to the reconstruction of past paleo-environmental changes in the marine realm that may have potentially resulted from climate changes on land. However, investigations addressing the behavior and uptake mechanism of Cr, and the potential isotope fractionations between seawater and biogenic carbonates are scarce. All studies so far conducted on marine biogenic carbonates have revealed the incorporation of isotopically lighter chromium into skeletal and non-skeletal carbonates

380   compared to Cr isotope signatures of seawater at the respective sampling sites (e.g., Pereira et al. (2015), Holmden et al. (2016); Farkaš et al., (in press)). Due to lack of ambient seawater δ^{53}Cr data to compare the ^{53}Cr data of various foraminifera analyzed by Wang et al. (2016), conclusion with respect to using δ^{53}Cr data of foraminiferal species as reliable proxy of seawater δ^{53}Cr could not be made in the respective study. However, these authors observed large δ^{53}Cr variations between species within

385   and among samples. Such variations in δ^{53}Cr among different samples could be explained by heterogeneous seawater δ^{53}Cr. However, Wang et al. (2016) also found that foraminifera species with similar depth habitats from the same core- top sample also yielded different δ^{53}Cr values. In addition,

15

within samples, foraminifera with shallower habitats yielded consistently lower δ^{53}Cr than those with deeper habitats, which these authors correctly described as opposite to the general patterns expected

390 in seawater δ^{53}Cr (Bonnand et al. (2013); Scheiderich et al.(2015); Paulukat et al. (2016)). The study of Farkaš et al.(in press) deals with chromium isotope variations in recent biogenic carbonates and ocean waters from Lady Elliot Island located in the southern Great Barrier Reef, Australia. The Cr isotope data from the Lady Elliot Island seawater-carbonate system, representing the South Pacific region, were complemented by δ^{53}Cr analyses of recent skeletal carbonates originating from the North Pacific,

395 North and South Atlantic Oceans, and from the Mediterranean Sea. The results of Farkaš et al. (in press), combined with the published seawater δ^{53}Cr data from the above oceanic water bodies, confirm the results of Pereira et al. (2015) that marine biogenic carbonates are systematically enriched in light Cr isotopes compared to ambient ocean waters. There is growing debate about the mechanisms inherent to Cr isotope fractionation during calcifying processes: Results published so far

400 point into a direction whereby vital processes (i.e., biology) could potentially play a major role in controlling Cr isotope fractionation during skeletal, foraminiferal, algal and shell calcification. The apparent variability of foraminiferal δ^{53}Cr values in the study of Wang et al. (2016) could be envisaged as to result from variable Cr uptake mechanisms. These authors propose, that in regions with high dissolved organic matter, foraminifera could preferentially uptake Cr(III) associated with dissolved

405 organic phases and/or organic matter, as observed for some phytoplankton (Semeniuk et al., 2016). In regions where dissolved organic concentration is low, foraminifera may switch to the reductive Cr(VI) uptake mechanism, as proposed for coral growth (Pereira et al., 2015). As Cr(III) is typically isotopically lighter than Cr(VI) in both equilibrium and kinetic fractionations (e.g., Ellis et al. (2002); Schauble et al. (2004); Wang et al. (2015)), Cr(III) uptake mechanism via organic matter would lead to relatively low

410 δ^{53}Cr values. A reductive Cr(VI) uptake mechanism is also expected to lead to lower- than- seawater δ^{53}Cr values in marine biogenic carbonate systems. In this case, the exact δ^{53}Cr value would depend on the extent of reduction and specific metabolism. A small extent of reduction would lead to low δ^{53}Cr values, while quantitative reduction would lead to similar to seawater values (Wang et al., 2016).

16

Direct incorporation of organic acid and/or siderophore bound Cr(III), as recently proposed by Saad et al. (2017) to have a significant impact on the Cr cycle via their release from the continents to the oceans, can also be considered to play a role in the marine biogenic calcification processes as these compounds have been shown to carry isotopically heavy Cr(III) compositions that are reached through redox-independent chromium isotope fractionation induced by ligand-promoted Cr(III) dissolution on land.

5.2 Surface seawater

The Playa Poniente seawater data are compatible with data from other Mediterranean surface seawaters, which distinguish in [Cr] vs. δ^{53}Cr space from Baltic Sea seawater, but are compatible with the trend of an inverse logarithmic relationship between δ^{53}Cr and [Cr] defined by Scheiderich et al. (2015) and substantiated later by Paulukat et al. (2016) of worldwide Atlantic and Pacific ocean waters. Three separate analyses of seawater from Disko Island, published by Paulukat et al. (2016), are characterized by slightly lower [Cr] and δ^{53}Cr values compared to the Mediterranean waters, but are similar to other waters from the North Atlantic (c.f., Fig. 2 in Paulukat et al. (2016)). Our data therefore support the hypothesis put forward by Scheiderich et al. (2015) that the observed Cr isotope signature in worldwide seawater likely arises from fractionation during the reduction of Cr(VI) in surface waters, scavenging of isotopically light Cr(III) to deeper water and sediment, and subsequent release of this seawater-derived Cr(III) back into seawater, either as organic complexes with Cr(III) or after oxidation to Cr(VI).

5.3. Shell transects

Placuna Placenta from Kininada Bay: We here attribute the exceptionally high Cr concentration in this sample to increased, organic-rich components which seem to act as efficient Cr hosts, basically

17

reflecting our experiments on *Mytilus edulis* from Godhavn (Fig. 5). Although some fluctuations in [Cr] and δ^{53}Cr values beyond the statistical errors across the beak-margin profile of the studied *Placuna placenta* specimen exist (which we may attribute to local (seasonal?) changes in seawater composition during growth and/or to changing reductive efficiencies during the calcification process), the studied specimen pretty much averages such environmental and biogenic changes out over its entire growth period estimated to be about 2 years. We here attribute the exceptionally high Cr concentration in the beak sample (CAP A) to increased, organic-rich components which seem to act as efficient Cr hosts, basically confirming our experiments on *Mytilus edulis* from Godhavn (Fig. 5). Chromium concentrations in this oyster from the Indian Ocean are comparable with those of the Mediterranean shells studied from Playa Poniente (Table 2, Fig. 4). In contrast, δ^{53}Cr values of *Placuna placenta* are lower than those recorded in the Mediterranean bivalves and show values that are just about statistically distinguishable from the igneous Earth inventory value of -0.12 +/- 0.11 ‰ defined by Schoenberg et al. (2008). Lack of a respective surface seawater sample from Kakinada Bay itself does not allow for a concrete definition of the Δ_{Cr} value- the nearest surface seawater sample from which we have a Cr isotope composition available is from the Bay of Bengal with δ^{53}Cr = 0.55 +/- 0.08 ‰ (Paulukat et al., 2015). If we assume that the local surface seawater in Kakinada Bay has a similar Cr isotope composition, then Δ_{Cr} would be ~0.5‰, an offset which is similar to that of *Loripes lucinalis* from Playa Poniente, but higher than most other species from this Mediterranean location.

Mimachlamys townsendi from Hawke's Bay: If Hawke's Bay surface seawater has a δ^{53}Cr similar to that of the Bengal Bay (Paulukat et al., (2015); and assuming it has remained about the same since the collection of the *Mimachlamys townsendi* sample), then *Mimachlamys townsendi* exhibits the same Δ_{cr} value (~0.5 ‰) as *Placuna placenta* from Kakinada Bay. If calcification processes in *Mimachlamys townsendi* remained constant in terms of biogenic reduction of Cr(VI) to isotopically lighter Cr(III) over the several years of growth of the specimen studied, then this would signify are more or less constant δ^{53}Cr of surface water in this location.

18

5.4~~2~~. Individual shells - ~~c~~Chromium distribution coefficients (D_{Cr}) between bivalve shell carbonates and seawater

470   Our sample sets from Playa Poniente and from Godhavn, which contain both surface seawater and bivalve shell data, allow for a direct calculation of the distribution coefficients (D_{Cr}) describing the partitioning of chromium between biogenic $CaCO_3$ and seawater at the respective study sites. The D_{Cr} is calculated as:

475        $D_{Cr} = ([Cr]_{CaCO3} / [Cr]_{seawater})$

where $[Cr]_{CaCO3}$ represents the measured total concentration of chromium in the bivalve shell (CaCO3 and organic matter hosted) and $[Cr]_{seawater}$ the measured dissolved chromium concentration of the

480   surface seawater at the respective location (e.g., 0.000300 ppm; 0.000176 ppm, and 0.000254 ppm, respectively, for Hawke's Bay/Kakinada Bay, Godhavn and Playa Poniente).

       The calculated D_{Cr} values for biogenic carbonates are listed in Table 2. Our data span a wide range with values from 70 to 1297, but the upper data limit is characterized by a few exceptionally high D_{Cr} values, f.e. that of sample Cap A (D_{Cr} = 1297) and Pec H (D_{Cr} = 820) from the respective hinges

485   of the *Placuna placenta* species from Kakinada Bay and the *Mimachlamys townsendi* specimen from Hawke's Bay which probably are characterized by elevated organic matter. By far most samples have a more restricted D_{Cr} range with values between 70 and 640. The D_{Cr} range presented herein for bivalves is much more narrow compared to data from the study of Farkaš et al. (in press) in which these authors present D_{Cr} values spanning more than three orders of magnitude (from 79 up to 10895) in

490   marine biogenic carbonates from Lady Elliot Island and other worldwide locations. However, as Farkaš et al.(in press) note, skeletal carbonates (i.e., corals, mollus~~k~~es) in their study tend to have

19

systematically lower values (from ~80 to ~780) than microbial carbonates (i.e., calcifying algae) that yielded much higher D_{Cr} of ~1000 and 2356. The range of D_{Cr} values for corals and mollus~~ke~~s in the study of Farkaš et al. (in press) otherwise compares well with the range of D_{Cr} values for bivalve shells in our study, and are within the range of D_{Cr} calculated for formanifera that vary from ~300 to 4000 (Wang et al., 2016) and with D_{Cr} values for corals in the range of 135 to 253 calculated from data in Pereira et al. (2015). Such high D_{Cr} values observed in biogenic carbonates produced by different marine organisms point to a strong biological control over the incorporation of Cr from seawater into $CaCO_3$ skeletons, where it could be incorporated either as Cr(III) and/or Cr(VI) depending on species-specific redox cycling of Cr (cf., Wang et al. (2016); Semeniuk et al. (2016)) and/or, as recently suggested, directly assimilated as organic ligand-bound Cr during biological uptake (Saad et al., 2017). It is too premature to compare the biogenic distribution coefficients with abiogenic values, simply because there is a lack of suitable modern seawater – carbonate pairs from which such values could be calculated. To our knowledge, the only suitable pair that allows for an estimation of a seawater-carbonate sediment distribution coefficient is that published by Holmden et al. (2016) for Jamaica. Using their average [Cr] of 140 ng/kg for Jamaican surface seawater and 9 ppm for Jamaican carbonate sediment (their Table 3), we calculate a D_{Cr} value of ~64'000. This value is significantly higher than D_{Cr} values from biogenic carbonates calculated in this study and from data in Farkaš et al. (in press), and possibly point to the potential discrimination of Cr against incorporation into marine calcifying skeletons.

5.~~3~~5 Evidence for isotopically fractioned Cr ~~incorporated~~ in bivalve shell carbonates

Our study confirms the outcome of previous investigations (Wang et al., 2016;Pereira et al., 2015;Farkaš et al., in press) showing that marine (skeletal and non-skeletal) biogenic carbonates are characterized by isotopically variably fractionated, but systematically [53]Cr enriched Cr compositions that have $\delta^{53}Cr$ values above the Earth's igneous inventory value of 0.12 +/- 0.11 ‰. From data which

20

allow direct comparison with ambient seawater compositions, including those presented in this study, it can also be deduced that the biogenic carbonates so far analyzed all have Cr isotope compositions

520 which are depleted in [53]Cr relative to respective seawater values, implying redox cycling, in particular reductive processes, to take place somewhere during the uptake and calcification processes.

In order to explain the isotopically light Cr incorporated in coral skeletal carbonate, Pereira et al. (2015) propose a mechanism whereby initial photoreduction of isotopically heavy Cr(VI) in the surface seawater to isotopically lighter Cr(III) in the endodermal layer of corals must be followed by

525 efficient and effective re-oxidation of reduced Cr species to favor subsequent chromate (CrO_4^{2-}) substitution during the calcifying processes ultimately leading to the coral skeleton.

~~To further test a possible role of biologically mediated redox processes during the incorporation of Cr from seawater into biogenic carbonate, Farkaš et al.(in press) investigated the relationship between δ^{53}Cr and cerium anomaly (Ce/Ce*) data in their biogenic carbonate samples~~

530 ~~from Lady Eliot Island. The strong and statistically significant negative correlation between Ce/Ce* and δ^{53}Cr data in their study, and the fact that the intercept of the δ^{53}Cr vs. Ce/Ce* correlation line overlaps with the Cr isotope composition of a local ocean water, led these authors to suggest that marine biogenic carbonates that precipitated from seawater and/or calcifying fluid under the most oxic conditions (i.e., having the most negative Ce/Ce*) can actually reflect the Cr isotope signature of~~

535 ~~ambient ocean water.~~

5.~~6~~4 Biomineralization / calcification and incorporation of chromium into shell~~s~~

A central question is that regarding the mechanisms on how dissolved chromium from

540 the seawater behaves during biomineralization and calcification processes, and ultimately is incorporated into marine biogenic carbonates. It becomes evident from recent studies (Wang et al., 2016;Pereira et al., 2015;Farkaš et al., in press) that redox mediated processes play a role during calcification because marine biogenic carbonates measured so far all are characterized by significantly

21

[53]Cr depleted (i.e., isotopically lighter) signatures relative to ambient seawaters. Reduction processes

545 of dissolved Cr(VI) complexes to Cr(III) species in ocean water have been used by Scheiderich et al.

(2015) and Paulukat et al. (2016) to explain the δ^{53}Cr variations in world's oceans. Scavenging of

isotopically light Cr(III) to deeper water and sediment, potentially by phytoplankton (Semeniuk et al.,

2016), and subsequent release of this seawater-derived Cr(III) back into seawater, either as organic

complexes with Cr(III) or after oxidation to Cr(VI), are advocated as potential processes to explain the

550 δ^{53}Cr *vs* [Cr] fractionation trend in seawater.

It is unclear, whether Cr can be directly incorporated into the carbonate structures as

Cr(VI) forming part of CrO_4^{2-} compounds, or whether reduced species of Cr(III) can be

assimilated/adsorbed or structurally bound into skeletal carbonates or associate with a multitude of

known organic matrices contained within and along cleave/grain boundaries of calcifying layer

555 carbonates. In one way or the other, models that address the mechanisms of Cr uptake during

calcification processes need to involve the fact that bulk marine biogenic carbonates are isotopically

lighter than ambient seawater in which they are formed. Pereira et al. (2015) proposed a model for

skeletal carbonates of corals whereby initial photoreduction of isotopically heavy Cr(VI) to isotopically

lighter Cr(III) in the endodermal layer of corals must be followed by efficient and effective re-oxidation

560 of reduced Cr species to favor subsequent chromate (CrO_4^{2-}) substitution during the calcifying

processes ultimately leading to the formation of the coral skeleton.

A vast number of studies dedicated to biomineralization processes of marine biogenic

carbonate producers have recognized the importance of organic network matrices (Griesshaber et al.,

2013), and of organic macromolecules in particular (e.g., (Suzuki et al., 2011;Okumura et al., 2013), in

565 the organic–inorganic interaction in biomineralization of, particularly, molluscan shells. Major

components of the shell are calcium carbonate, which ordinarily exists as a crystalline polymorph,

either calcite or aragonite. The type of polymorph, crystal orientation, morphology and texture of the

crystals are regulated in the shell. Studies have shown that shells are not composed of purely inorganic

carbonate crystals, but contain small amounts of organic substances to regulate the structure and

570　property of these crystals (e.g., (Falini et al., 1996;Belcher et al., 1996;Okumura et al., 2013). Suzuki et al. (2011) visualized intra-crystalline spherular structures in shell carbonates containing carbon from organic macromolecules. The size of the spherules identified by these authors roughly corresponded to that of soluble organic macromolecules that these authors extracted from the nacreous layer (innermost layer of the shell of a mollusk secreted by the mantle epithelium layer). Their function for

575　the crystal formation of molluscan shells remains unclear though. A comprehensive review on the presence and role of organic matrices for the growth of mollusk shells is contained in Suzuki and Nagasawa (2013).

~~While recognizing that individual processes leading to the presence of various organic compounds in mollusk shell calcification and growth, and biomineralization processes are complex and~~

580　~~topic of intensified research in the last years,~~W we like to focus our attention on the potential role of ~~such~~ organic matrices as hosts for Cr in mollusk shells. A hint that organics may play a defining role stems from our few results which compare [Cr] in <u>incinerated</u> shell material ~~that has been incinerated~~ to corresponding [Cr] in aliquots which were attacked with *aqua regia* to preferentially attack the carbonate. While it is clear from our study of *Mytilus edulis* from Godhavn with an apparent organic-

585　rich periostracum that this outermost shell layer itself may contain elevated [Cr], based on a similar result (c.f., Fig. 3, Table 2) performed on *Loripes lucinalis* from Playa Poniente where the actual periostractum has been mechanically removed by tidal abrasion in the beach sand, we suspect that organics contained in the nacreous layer are equally important as potential Cr hosts. In all cases (see above and Table 2) we note significantly higher [Cr] in the ashed samples, which we see as a

590　consequence of effective release of organic-material bound Cr (otherwise only weakly- or even not attacked at all by the hydrochloric acid) during burning of the organic material. So, for example, Suzuki et al. (2007) hydrolyzed the insoluble organic matrices from the prismatic layer in the mollusk shell with 6 M HCl. These authors detected D-glucosamine hydrochloride, known as a degradation product of chitin, using nuclear magnetic resonance spectroscopy measurements. In the nacreous layer of

595　mollusk shells, chitin serves as the major component of the organic framework, building up the

23

compartment structure and controlling the morphology of calcium carbonate crystals (Falini and Fermani, 2004).

5.7~~5~~ A model explaining the occurrence of Cr in molluscan shells

Adopting the schematic framework that includes the representation of the localization and function of organic matrices with respect to calcium carbonate crystals in the nacreous layer of mollusks we like to propose a model that explains the transfer of Cr from the water into the calcifying space and the incorporation of Cr into shell carbonates (Fig. 8). During adult shell formation, the periostracum, which is not mineralized and covers the external surface of the shell, is formed first, and the calcified layer subsequently forms on the periostracum (e.g., (Checa, 2000)). The shell is in contact with the mantle, which supplies the periostracum and calcified layers with inorganic ions and organic matrices through the extrapallial fluid (for a review, see Marin et al. (2012)). ~~This extrapallial space is supposed to be the confined medium where all the ingredients for calcification self-assemble. The extrapallial fluid, filling this space, is supersaturated with respect to calcium carbonate. In addition to the precursors ions for mineralization – calcium and bicarbonate – this fluid contains several other inorganic ions, such as Na^+, K^+, Mg^{2+}, Cl^- and SO_4^{2-}, and minor elements, such as Sr and Fe. Its pH is usually slightly basic, in the range of 7.4 – 8.3, for marine and freshwater mollusks (Marin et al., 2012).~~ This fluid also contains organic molecules. As the fluid is supersaturated with respect to calcium carbonate, these macromolecules – in particular acidic proteins and GAGs (group specific antigen) - are supposed to transiently maintain calcium in solution, by inhibiting the precipitation of calcium carbonate, and by allowing it to precipitate where needed (Marin et al., 2012). The manner the inorganic precursors of calcification are driven to the site of mineralization is still speculative. Figure 8 schematically shows the growth front in an interlamellar space of the nacreous layer, confined by chitinous membranes, as proposed by Suzuki and Nagasawa (2013). We emphasize that under neutral to basic pH, as inferred for an extrapallial fluid, Cr is present either as dissolved Cr(VI) compound, as

Cr(III) species adsorbed onto organic macromolecules and/or as dissolved organic substances. The fact that δ^{53}Cr measured in bivalve shells is systematically lower than ambient seawater implies that reduction of dissolved Cr(VI) in seawater, transferred to the calcifying space , is likely promoted by the organic macromolecules, which are densely localized on the surface of the interlamellar membranes (Suzuki and Nagasawa, 2013;Suzuki et al., 2011). So-formed isotopically light Cr(III) species, effectively adsorbed onto organic macromolecules, adhere to the chitinous membranes where they are incorporated inside growing carbonate crystals filling the space, whereas other organic molecules cover the surface of these crystals. Finally, surface-covering organic macromolecules are also incorporated inside the crystal when the space is filled with the crystal. Some Cr might also be directly incorporated into the carbonate lattices during growth, where chromate ions may coprecipitate with calcite (Tang et al., 2007). In such a scenario, the measured bulk δ^{53}Cr values of mollusk shells would reflect a mixture of both Cr(VI) and Cr(III) characteristic of the ambient seawater and an isotopically lighter, Cr(III) fraction ultimately associated with the organic molecules in the shells. The exact δ^{53}Cr value would depend on the extent of reduction and specific metabolism. A small extent of reduction would lead to low δ^{53}Cr values while quantitative reduction of dissolved Cr(VI) would lead to similar to seawater values.

5.86 Inter-and intra-species shell variations

While from the studies conducted earlier (e.g., (Pereira et al., 2015;Wang et al., 2016) and from this study it is now evident that marine biogenic carbonates are characterized by δ^{53}Cr values that are less fractionated comparedin comparison to ambient seawater, it remains unclear whether these isotopic offsets are species dependent. Wang et al. (2016) observed large δ^{53}Cr variations between foraminifera species within and among samples. As advocated by these authors, the variation in δ^{53}Cr among different samples of the same species could be explained by heterogeneous seawater δ^{53}Cr. However, Wang et al. (2016) also found that foraminifera species with

25

similar depth habitats from the same core- top sample also yielded different δ^{53}Cr values. Species

dependent δ^{53}Cr variations are furthermore complicated by the observation that species with

650   shallower water depth habitats yielded consistently lower δ^{53}Cr than species preferring deeper water

environments, which is opposite to the general patterns expected in seawater δ^{53}Cr (Bonnand et al.,

2013;Scheiderich et al., 2015). These observations hint at the possibility that species-dependent

biological (metabolic) processes may play a major control on Cr isotope fractionation during

biomineralization/calcification processes of marine biogenic carbonate producers in general, not only

655   in foraminiferal calcification. Our data herein contribute to a more systematic assessment of the

above: The systematic sampling of some bivalve species from the same location over several years,

together with respective ambient surface seawaters, reveals that subtle inter-species differences of

average bulk δ^{53}Cr signatures exist amongst different species. While 5 species (*Calista chione*, an

unidentified species of Cardiidae, *Chamelea striulata*, *Glycymeris glycymeris*, and *Pecten jacobaeus*)

660   however, at the 2σ level, cannot be statistically distinguished by their average δ^{53}Cr values (Fig. 3),

Loripes luncinalis is an exception and yielded, at average, lower δ^{53}Cr values than the other species.

Thus, while we observe subtle differences in the average δ^{53}Cr signatures of individual bivalve species

from Playa Poniente, intra-species variations, as observed by Wang et al. (2016) for certain

foraminifera, are statistically not discernable. The exception to this are two samples of *Arca*

665   *Navicularis*, sampled simultaneously in 2015, which both show distinctly different δ^{53}Cr signatures of

0.570 and 0.166 ‰, and also significantly different [Cr] of 0.052 and 0.166 ppm, respectively. We are

unable, at this point, to explain these discrepancies observed in *Arca Navicularis*. Last not but least,

while [Cr] in the samples studied scatter considerably between ~0.03 to 0.10 ppm and do not correlate

with bivalve species, there is an exception to this which is reflected by the data of *Pecten jacobaeus*.

670   The three samples of this species all revealed elevated [Cr] in the range of 0.127 to 0.163 ppm (Table

2, Fig. 3). Whether or not the intensity of pigmentation (*Pecten jacobaeus* shows a red pigmentation

that increases from the hinge to the margin of the shell; Fig. 2) is not clear, but it could partially

explain the increased [Cr] scatter in the analyses from *Glycymeris glycymeris* (c.f., Fig. 2, Table 2) which

26

exhibits similar variations in pigmentation amongst individual samples. Importantly, however, is the fact that the increased scatter of [Cr] does not seem to translate into an increased scatter of bulk δ^{53}Cr values of the bivalve shells studies, nor does [Cr] seem to correlate with δ^{53}Cr in any of the species studied either. If, as emphasized in our preferred scenario, that [Cr] in the bivalve shell is significantly associated with organic matter, it implies that intralamellar reductive processes eventually lead~~ing~~ to adsorption of isotopically light Cr(III) onto organic macromolecules. The~~, and the~~ production rate of these macromolecules~~,~~ are likely metabolically controlled/buffered prior to their encapsulation into the shell carbonates. This is maybe best exemplified by the *Mytilus edulis* sample suite from Godhavn. This suite of samples reveals limited intra-species variations both in δ^{53}Cr and [Cr] among the 6 half-shells analyzed, which we take as an indication for an effective and stabilizing biological control, potentially via organic macromolecule production, of biomineralization processes in general, and of Cr incorporation into the shell carbonates.

Our study may eventually also contribute to the understanding of the environmental stability over relevant growth periods (several years) around the calcifying space of bivalves. However, such investigations are dependent on the knowledge of the seawater Cr isotope composition during the respective growth periods (in our case during growth of the *Placuna placenta* from Kakinada Bay and the *Mimachlamys townsendi* sample form Hawke's Beach, which we do not have at hand. It is strongly perceivable that surface seawater conditions at a specific location are not, and have not been constant, and this has been shown for the δ^{53}Cr values of surface water from the Baltic Sea by Paulukat et al. (2016). These authors correlated seasonal fluctuations in δ^{53}Cr with algae bloom periods, and thus with the seasonal presence of strong Cr(VI) reducers capable of depleting the [Cr] in the surface waters considerably by reductive adsorption mechanisms. Seasonal fluctuations could explain the sinusoidal δ^{53}Cr growth pattern in the studied *Placuna placenta* shell (Fig. 6) whose size roughly implies a ~1 year's growth period. Likewise, small fluctuations in *Mimachlamys townsendi* of δ^{53}Cr signatures over the entire growth period of the specimen studied could reflect seasonal changes of the ambient surface seawater during this several years long growth period. We however want to

27

emphasize that these within- shell δ^{53}Cr fluctuations, in the order of +/- 0.15‰, compare well with inter-species fluctuations of the same order observed in all the Playa Poniente bivalve species. This makes the average δ^{53}Cr signature of a bivalve shell still a valuable parameter which, given that the isotopic offset from ambient seawater is known, potentially can be used for recording the seawater Cr isotope signature prevailing at the habitat location of the respective bivalve.

705

5.9̶7̶ A first attempt to define average δ^{53}Cr offsets of specific bivalves from ambient seawater

Our data set allow for a preliminary definition of Cr isotope offsets between certain bivalve species and ambient seawater, which potentially could be used in paleo-seawater

710 reconstructions using suitable fossil aliquots. Instead of using average δ^{53}Cr values defined by our sample suites, and average seawater δ^{53}Cr values, we prefer to define such offsets (Δ_{Cr}) conservatively, using band widths (rather than comparing average values) that take analytical uncertainty into consideration (i.e., minimum Δ_{Cr} values defined by difference between (δ^{53}Cr + 2σ)$_{sample}$ and (δ^{53}Cr − 2σ)$_{seawater}$; maximium Δ_{Cr} values defined by difference between (δ^{53}Cr - 2σ)$_{sample}$ and (δ^{53}Cr +

715 2σ)$_{seawater}$). These ranges are listed in Table 3 and plotted in Figure 9 for all species where we have multiple analyses and ambient seawater values. The Δ_{Cr} offset range of *Placuna placenta* is not strictly comparable to the other values as it includes growth segment analyses covering the growth period of the entire shell. These introduce enhanced scatter that is most likely due to seasonal changes of seawater, a factor which is smoothed out by the analyses of entire shells as is the case for the other

720 species. This explains the rather large Δ_{Cr} range calculated for *Placuna placenta*.

Although preliminary (additional data need to be collected to more precisely define species dependent ranges), our data allow for a first order estimation on the use of the Δ_{Cr} seawater offset ranges defined herein to ultimately reconstruct the local surface seawater redox state. On̲A̶t̶ average, δ^{53}Cr values of ambient seawater can be reconstructed to ~+/- 0.3 ‰. At first sight, this

725 seems to be rather imprecise, but considering that surface seawaters today exhibit δ^{53}Cr variations

between +0.13‰ and +1.24‰ (Paulukat et al., 2016), this uncertainty nevertheless allows for placing reconstructed seawater compositions into a meaningful redox framework. The usefulness of this tool for the reconstruction of paleo-seawater compositional changes awaits the assessment, testing and acquisition of Cr isotope composition of fossil calcifiers that can be compared to data from modern

730   respective species.

6. Conclusions

We have conducted bulk δ^{53}Cr and [Cr] analyses of a set of common bivalve species from

735   two locations, one at Playa Poniente on the Mediterranean Sea, and one from Disko Bay in arctic north Atlantic, from where we also measured the ambient seawater. Collection of same species during a specific period in July over several years, and of multiple samples from some of the species, allowed us to monitor the stability of Cr isotope signatures in each of the species, and to define long-term δ^{53}Cr offsets from ambient seawater. The outcome of our study can be summarized as follows:

740   1. The local surface seawater Cr isotope composition and [Cr] concentrations at Playa Poniente at times of sample collection over a three years period is surprisingly homogenous, with δ^{53}Cr = 0.83 +/- 0.05 ‰, and with [Cr] = 254 +/- 54 ng/kg.

      2. Offsets (Δ_{Cr}) from different bivalve species from this value show subtle differences, with typical values of ~0.3 to 0.4 ‰ lower than ambient seawater. Of all the species

745   investigated, *Loripes lucinalis* exhibits the largest Δ_{Cr} of ~0.6 ‰. The systematically lighter Cr isotope compositions of all bivalves studies herein relative to ambient seawater confirms earlier studies by Pereira et al. (2015) on corals, by Wang et al. (2016) on foraminifera, and by Farkaš et al. (in press) for various marine calcifiers from a location in the Barrier Reef.

750   3. Recognizing the importance of organics in the shell structures of bivalves, and considering our results from incinerated *vs*. solely 6N HCl dissolved bivalve shells

systematically showing recovery of higher [Cr] in ashed samples, we propose a model whereby reduction of Cr(VI) originally contained in the seawater and transported to the calcifying space, to Cr(III), and its effective adsorption onto organic

755   macromolecules that adhere to chitinous interlameallar coatings, plays a central role. In such a scenario, organic matter-bound, isotopically light Cr, forms preferable loci for the nucleation of carbonates, and it is eventually included into the growing shell carbonates, possible together with dissolved chromate that may substitute for CO_3^{2-} directly in the carbonate lattice.

760   4. Inter-species Cr isotope variations, tested on a suite of contemporaneously sampled alive *Mytilus edulis* samples from Godthavn (Disko Bay), are small, in the range of $\delta^{53}Cr$ = +/- 0.05 ‰, and independent of [Cr]. Although not knowing the exact host of Cr in these shells (periostracum, organic macromolecules, chitinous interlamellar membranes ? etc.), the homogenous Cr isotope composition measured in this suite of

765   samples renders *Mytilus edulis* a potential archive for the reconstruction of the redox state of ambient local seawater. This needs to be verified by studies of this species from other locations before attempts to use fossil aliquots for the reconstruction of paleo-seawater redox.

5. Intra-shell variations of $\delta^{53}Cr$ and [Cr] over respective entire growth periods was

770   investigated on two examples, a sample of *Placuna placenta* (window pane oyster, Capiz) and a sample of *Mimachlamys townsendi* (Pecinidae), from Kakinada Bay (Bay of Bengal) and from Hawke's Beach (Karachi, Pakistan). We observe subtle fluctuation of both parameters of the growth period of ~1 year and several years, respectively, which are in the order of 0.1 to 0.2 ‰. These fluctuations may arise from either

775   seasonal changes in ambient seawater compositions, and/or from metabolic instabilities in the calcifying space affecting reduction of Cr(VI) and production of organic macromolecules.

6. Our study can be used as a base for futures, more detailed investigations of marine biogenic carbonates, including fossil marine calcifiers, aimed at the reconstruction of paleo-seawater redox state fluctuations, and eventually to correlate these with climate change aspects in certain periods of Earth's history.

Author contribution

RF initiated the study and collected the samples, RF and CP processed the samples through the chemistry and performed the mass spectrometrical analyses, and continuous discussions through the lengthy project period amongst all co-authors (RF, CP, SB and RK) led to substantial improvement, enhanced understanding, important modifications and adaptations of the original research ideas. RF prepared the manuscript with contributions from all co-authors.

31

805

Figure captions

Figure 1.

810 World sketch map with locations from where bivalve and seawater samples were collected.

Figure 2.

Photographs of representative bivalve species studied herein. 1-8 from Playa Poniente, 9 from

Kakinada Bay, 10 from Hawke's Bay, and 11 from Godhavn (Qeqertarsuaq). Black scale line

815 corresponds to 1 cm.

1.Cardiidae (unknown species); 2. *Pecten jacobaeus*; 3. *Challista chione*; 4. *Glycymeris glycymeris*; 5.

Chamelea striulata; 6. *Loripes lucinalis*, 7. *Venus verrucosa*; 8. *Arca navicularis*; 9. *Placuna placenta*

(window pane oyster, Capiz; with growth profile samples indicated); 10. *Mimachlamys townsendi*

(with growth profile samples indicated); 11. *Mytilus edulis*.

820

Figure 3.

Plot depicting average δ^{53}Cr values from multiple filament runs with 200 nanogram loads of NIST SRM

979 measured on the PHOENIX thermal ionization mass spectrometer at 53Cr beam intensities of

350mV and 1V, respectively. The yellow colored range indicates the +/- 0.08 ‰ external

825 reproducibility of the 10 filaments loads ran at 350mV 53Cr beam intensities, which correspond to

typical beam intensities obtained from our samples.

Figure 4.

Plot showing the chromium concentrations ([Cr]; blue filled symbols) and chromium isotope

830 compositions (δ^{53}Cr; red filled symbols) of various incinerated bivalve species analyzed from Playa

33

Poniente. 1 *Callista Chione*; 2 Cardiidae (species unknown); 3 *Chamelea gallina*; 4 *Chamelea striatula*; 5 *Glycymeris glycymeris*; 6 *Loripes lucinalis*; 7 *Pecten jacobaeus*; 8 *Venus verrucosa*. Stippled red lines mark the average values of inter-species analyses, the red ranges the two standard deviation errors of these analyses. The light gray horizontal bar depicts the Igneous Earth inventory composition

835 (Schoenberg et al., 2009), and the blue horizontal bar the local surface seawater composition measured from this location. One sample of *Loripes lucinalis* (marked with a light red - and a light blue filled symbol) has been dissolved in *aqua regia* without previous incineration. For details see text.

Figure 5.

840 Plot showing the chromium concentrations ([Cr]; blue filled symbols) and chromium isotope compositions (δ^{53}Cr; red filled symbols) of various *Mytilus edulis* shells and ~~a~~ of a shell mixture from Godhavn, Disko Bay, Greenland. The darker red - and darker blue filled symbol mark analyses on incinerated shells, whereas the lighter colored respective symbols depict analyses from solely *aqua regia* dissolved shells. The light gray horizontal bar depicts the Igneous Earth inventory composition

845 (Schoenberg et al., 2009), and the blue horizontal bar the local surface seawater composition measured from this location (Paulukat et al., 2016). For details see text.

Figure 6.

Plot showing the chromium concentrations ([Cr]; blue filled symbols) and chromium isotope

850 compositions (δ^{53}Cr; red filled symbols) of samples along a growth transect of a *Placuna placenta* sample (depicted in Fig. 2) from Kakinada Bay. Sample Cap-A is characterized by an elevated [Cr] which is potentially due an elevated organic content in the initial growth zone comprising the apex of the shell. The sinusoidal distribution of δ^{53}Cr values along the transect potentially reflects seasonal changes of ambient surface seawater. For details refer to text.

855

Figure 7.

34

Plot showing the chromium concentrations ([Cr]; blue filled symbols) and chromium isotope compositions ($\delta^{53}Cr$; red filled symbols) of samples along a growth transect in a *Mimachlamys townsendi* specimen from Hawke's Bay. Sample Pec-H is characterized by an elevated [Cr] which is potentially due an elevated organic content in the initial growth zone comprising the apex/hinge of the shell (c.f., Fig. 2). For details refer to text.

Figure 8.

Schematic representation of a simplified model for the transfer of chromium from an extrapallial fluid within an interlamellar space into shell carbonate nuclides (modified from Suzuki and Nagasawa, 2013). The insoluble frameworks consist of chitin (black and long rectangles) that make a scaffold to supply the space for precipitation of calcium carbonate crystals. A. The interlamellar space is filled with a supersaturated extrapallial fluid with respect to CO_3^{2-} and Ca^{2+}. Cr(VI) likely occurs as dissolved compounds in the fluid and eventually is reduced to isotopically lighter Cr(III) by dissolved organic macro-molecules (gray circles) onto which it is efficiently adsorbed. Insoluble matrix proteins (gray discs) have the hydrophobic region for organic macro-molecule (protein)–chitin interaction and the hydrophilic–acidic region for the calcium carbonate binding ability mediate the connection between the organic scaffolds. B. The soluble matrix proteins that have hydrophyllic region for calcium carbonate binding adhere to the chitinous layers and probably regulate nucleation, crystal polymorph and crystal orientation of inorganic calcium carbonate crystals (gray rectangles). C. As the crystals grow, insoluble matrix proteins are used for organic framework formation as intercrystalline organic matrices and soluble matrix proteins, including adsorbed Cr(III), are eventually included in the calcium carbonate crystals as intracrystalline organic matrices. Cr(VI) potentially present as chromate (CrO_4^{2-}) ions likely also substitute for carbonate (CO_3^{2-}) ions directly in the calcium carbonate lattice (Tang et al., 2009).

Figure 9. Bar graph showing the conservative offset ranges (Δ_{Cr}) of δ^{53}Cr values of bivalve species from ambient seawater. The larger range of *Placuna placenta* is due to within-shell heterogeneities probably resulting from seasonal surface seawater fluctuations which are smoothed out by the bulk
885   shell analyses of the other species (see text for details).

References

Beaver, P. E., Bucher, D. J., and Joannes-Boyau, R.: Growth patterns of three bivalve species targeted by the
890   Ocean Cockle Fishery, southern New South Wales: Eucrassatella kingicola (Lamarck, 1805); Glycymeris grayana
(Dunker, 1857); and Callista (Notocallista) kingii (Gray, 1827), Molluscan Research, 37, 104-112, 2017.

Belcher, A. M., Wu, X. H., Christensen, R. J., Hansma, P. K., Stucky, G. D., and Morse, D. E.: Control of crystal
phase switching and orientation by soluble mollusc-shell proteins, Nature, 381, 56-58, 1996.

Bonnand, P., Parkinson, I. J., James, R. H., Karjalainen, A.-M., and Fehr, M. A.: Accurate and precise
895   determination fo stable Cr isotope compositions in carbonates by double spike MC-ICP-MS, J. Anal. At.
Spectrom., 26, 528-536, 2011.

Bonnand, P., James, R. H., Parkinson, I. J., Connelly, D. P., and Fairchild, I. J.: The chromium isotopic composition
of seawater and marine carbonates, Earth Planet. Sci. Lett., 382, 10-20, 2013.

Checa, A.: A new model for periostracum and shell formation in Unionidae (Bivalvia, Mollusca), Tissue & Cell,
900   32, 405-416, 2000.

D'Arcy, J., Gilleaudeau, G. J., Peralta, S., Gaucher, C., and Frei, R.: Redox fluctuations in the Early Ordovician
oceans: An insight from chromium stable isotopes, Chem. Geol., 448, 1-12, 2017.

Døssing, L. N., Dideriksen, K., Stipp, S. L. S., and Frei, R.: Reduction of hexavalent chromium by ferrous iron: A
process of chromium isotope fractionation and its relevance to natural environments, Chem. Geol., 285, 157-
905   166, 2011.

Ellis, A. S., Johnson, T. M., and Bullen, T. D.: Chromium isotopes and the fate of hexavalent chromium in the
environment, Science, 295, 2060-2062, 2002.

Falini, G., Albeck, S., Weiner, S., and Addadi, L.: Control of aragonite or calcite polymorphism by mollusk shell
macromolecules, Science, 271, 67-69, 1996.

910   Falini, G., and Fermani, S.: Chitin mineralization, Tissue Eng., 10, 1-6, 2004.

Farkaš, J., Frýda, J., Paulukat, C., Hathorne, E., Matoušková, Š., Rohovec, J., Frýdová, B., Francová, M., and Frei,
R.: Chromium isotope fractionation between modern seawater and biogenic carbonates from the Great Barrier
Reef, Australia: Implications for the paleo-seawater $\delta^{53}Cr$ reconstructions, Earth Planet. Sci. Lett., in press.

Frei, R., Gaucher, C., Poulton, S. W., and Canfield, D. E.: Fluctuations in Precambrian atmospheric oxygenation
915   recorded by chromium isotopes, Nature, 461, 250-253, 2009.

Frei, R., Gaucher, C., Dossing, L. N., and Sial, A. N.: Chromium isotopes in carbonates - A tracer for climate
change and for reconstructing the redox state of ancient seawater, Earth Planet. Sci. Lett., 312, 114-125, 2011.

Frei, R., Gaucher, C., Stolper, D., and Canfield, D. E.: Fluctuations in late Neoproterozoic atmospheric oxidation -
Cr isotope chemostratigraphy and iron speciation of the late Ediacaran lower Arroyo del Soldado Group
920   (Uruguay), Gondwana Research, 23, 797-811, 2013.

Frei, R., Crowe, S. A., Bau, M., Polat, A., Fowle, D. A., and Dossing, L. N.: Oxidative elemental cycling under the
low O_2 Eoarchean atmosphere, Scientific Reports, 6, 21058, 2016.

Gerstenberger, H., and Haase, G.: A highly effective emitter substance for mass spectrometric Pb isotope ratio
determinations, Chem. Geol., 136, 309-312, 1997.

925   Gilleaudeau, G. J., Frei, R., Kaufman, A. J., Kah, L. C., Azmy, K., Bartley, J. K., Chernyavskiy, P., and Knoll, A. H.:
Oxygenation of the mid-Proterozoic atmosphere: clues from chromium isotopes in carbonates, Geochemical
Perspectives Letters, 2, 178-186, 2016.

Griesshaber, E., Schmahl, W. W., Ubhi, H. S., Huber, J., Nindiyasari, F., Maier, B., and Ziegler, A.: Homoepitaxial meso- and microscale crystal co-orientation and organic matrix network structure in Mytilus edulis nacre and calcite, Acta Biomaterialia, 9, 9492-9502, 2013.

930

Holmden, C., Jacobson, A. D., Sageman, B. B., and Hurtgen, M. T.: Response of the Cr isotope proxy to Cretaceous Ocean Anoxic Event 2 in a pelagic carbonate succession from the Western Interior Seaway, Geochim. Cosmochim. Acta, 186, 277-295, 2016.

Marin, F., Le Roy, N., and Marie, B.: The formation and mineralization of mollusk shell, Frontiers in Bioscience, S4, 1099-1125, 2012.

935

Minchin, D.: Introductions: some biological and ecological characteristics of scallops, Aquatic Living Resources, 16, 521-532, 2003.

Moura, P., Gaspar, M. B., and Monteiro, C. C.: Age determination and growth rate of a Callista chione population from the southwestern coast of Portugal, Aquatic Biology, 5, 97-106, 2009.

940

Murthy, V. S. R., Narasimham, K. A., and Venugopalam, W.: Survey of windowpane oyster (Placenta placenta) resources in the Kakinada Bay, Indian Journal of Fishery, 26, 125-132, 1979.

Okumura, T., Suzuki, M., Nagasawa, H., and Kogure, T.: Microstructural control of calcite via incorporation of intracrystalline organic molecules in shells, J. Cryst. Growth, 381, 114-120, 2013.

Paulukat, C., Dossing, L. N., Mondal, S. K., Voegelin, A. R., and Frei, R.: Oxidative release of chromium from

945

Archean ultramafic rocks, its transport and environmental impact - A Cr isotope perspective on the Sukinda valley ore district (Orissa, India), Appl. Geochem., 59, 125-138, 2015.

Paulukat, C., Gilleaudeau, G. J., Chernyavskiy, P., and Frei, R.: The Cr-isotope signature of surface seawater - A global perspective, Chem. Geol., 444, 101-109, 2016.

Pereira, N. S., Voegelin, A. R., Paulukat, C., Sial, A. N., Ferreira, V. P., and Frei, R.: Chromium-isotope signatures

950

in scleractinian corals from the Rocas Atoll, Tropical South Atlantic, Geobiology, 14, 54-67, 2015.

Planavsky, N. J., Reinhard, C. T., Wang, X. L., Thomson, D., McGoldrick, P., Rainbird, R. H., Johnson, T., Fischer, W. W., and Lyons, T. W.: Low Mid-Proterozoic atmospheric oxygen levels and the delayed rise of animals, Science, 346, 635-638, 2014.

Rodler, A., Sanchez-Pastor, N., Fernandez-Diaz, L., and Frei, R.: Fractionation behavior of chromium isotopes

955

during coprecipitation with calcium carbonate: Implications for their use as paleoclimatic proxy, Geochim. Cosmochim. Acta, 164, 221-235, 2015.

Rodler, A. S., Frei, R., Gaucher, C., and Germs, G. J. B.: Chromium isotope, REE and redox-sensitive trace element chemostratigraphy across the late Neoproterozoic Ghaub glaciation, Otavi Group, Namibia, Precambrian Res., 286, 234-249, 2016a.

960

Rodler, A. S., Hohl, S. V., Guo, Q., and Frei, R.: Chromium isotope stratigraphy of Ediacaran cap dolostones, Doushantuo Formation, South China, Chem. Geol., 436, 24-34, 2016b.

Saad, E. M., Wang, X. L., Planavsky, N. J., Reinhard, C. T., and Tang, Y. Z.: Redox-independent chromium isotope fractionation induced by ligand-promoted dissolution, Nature Communications, 8, 2017.

Schauble, E., Rossman, G. R., and Taylor, H. P.: Theoretical estimates of equilibrium chromium-isotope

965

fractionations, Chem. Geol., 205, 99-114, 2004.

Scheiderich, K., Amini, M., Holmden, C., and Francois, R.: Global variability of chromium isotopes in seawater demonstrated by Pacific, Atlantic, and Arctic Ocean samples, Earth Planet. Sci. Lett., 423, 87-97, 2015.

Schoenberg, R., Zink, S., Staubwasser, M., and von Blanckenburg, F.: The stable Cr isotope inventory of solid Earth reservoirs determined by double spike MC-ICP-MS, Chem. Geol., 249, 294-306, 2008.

970   Seed, R., and Suchanek, T. H.: Population and community ecology of Mytilus, in: The mussel Mytilus: ecology, physiology, genetics and culture, edited by: EM, G., Elsevier Science Publ., Amsterdam, 87-169, 1992.

Semeniuk, D. M., Maldonado, M. T., and Jaccard, S. L.: Chromium uptake and adsorption in marine phytoplankton - Implications for the marine chromium cycle, Geochim. Cosmochim. Acta, 184, 41-54, 2016.

Suzuki, M., Okumura, T., Nagasawa, H., and Kogure, T.: Localization of intracrystalline organic macromolecules

975   in mollusk shells, J. Cryst. Growth, 337, 24-29, 2011.

Suzuki, M., and Nagasawa, H.: Mollusk shell structures and their formation mechanism, Canadian Journal of Zoology-Revue Canadienne De Zoologie, 91, 349-366, 2013.

Tang, Y., Elzinga, E. J., Lee, Y. J., and Reeder, R. J.: Coprecipitation of chromate with calcite: batch experiments and X-ray absorption spectroscopy, Geochim. Cosmochim. Acta, 71, 1480-1493, 2007.

980   Trinquier, A., Birck, J. L., and Allegre, C. J.: High-precision analysis of chromium isotopes in terrestrial and meteorite samples by thermal ionization mass spectrometry, J. Anal. At. Spectrom., 23, 1565-1574, 2008.

Wang, X. L., Johnson, T. M., and Ellis, A. S.: Equilibrium isotopic fractionation and isotopic exchange kinetics between Cr(III) and Cr(VI), Geochim. Cosmochim. Acta, 153, 72-90, 2015.

Wang, X. L., Planavsky, N. J., Hull, P. M., Tripati, A. E., Zou, H. J., Elder, L., and Henehan, M.: Chromium isotopic

985   composition of core-top planktonic foraminifera, Geobiology, 15, 51-64, 2016.

Yamaoka, Y., Kondo, Y., and Ito, H.: Rate and pattern of shell growth of *Glycymeris fulgurata* and *Glycymeris vestita* (Bivalvia: Glycymerididae) in Tosa Bay as inferred from oxygen isotope analysis, Venus, 74, 61-69, 2016.

Zink, S., Schoenberg, R., and Staubwasser, M.: Isotopic fractionation and reaction kinetics between Cr(III) and Cr(VI) in aqueous media, Geochim. Cosmochim. Acta, 74, 5729-5745, 2010.

990

AUTHOR QUERY FORM

Dear Author,

Please check your proof carefully and mark all corrections at the appropriate place in the proof. **It is crucial that you NOT make direct edits to the PDF using the editing tools as doing so could lead us to overlook your desired changes.** Rather, please request corrections by using the tools in the Comment pane to annotate the PDF and call out the changes you would like to see. To ensure fast publication of your paper please return your corrections within 48 hours.

For correction or revision of any artwork, please consult *http://www.elsevier.com/artworkinstructions*

Any queries or remarks that have arisen during the processing of your manuscript are listed below and highlighted by flags in the proof.

Location in article	Query / Remark: **Click on the Q link** to find the query's location in text Please insert your reply or correction at the corresponding line in the proof
Q1	Your article is registered as a regular item and is being processed for inclusion in a regular issue of the journal. If this is NOT correct and your article belongs to a Special Issue/Collection please contact <f.kay@elsevier.com> immediately prior to returning your corrections. (p. 1/ line 1)
Q2	The author names have been tagged as given names and surnames (surnames are highlighted in teal color). Please confirm if they have been identified correctly and are presented in the desired order. (p. 1/ line 17)
Q3	Please indicate which author(s) should be marked as 'Corresponding author'. (p. 1/ line 18)
Q4	The number of keywords provided exceeds the maximum of 6 allowed by this journal. Please provide the final list of 6 keywords for the article. (p. 1/ line 37)
Q5	Please check the e-mail address that has been added here, and correct if necessary. (p. 1/ line 62)
Q6	Figure(s) will appear in black and white in print and in color on the web. The figure(s) contains references to color or the colors are mentioned in the main text. Based on this, the explanatory text about the interpretation of the colors has been added. Please check, and correct if necessary. (p. 3/ line 50)
Q7	Please check if sponsor names have been identified correctly and correct if necessary. (p. 14/ line 5)
Q8	Please provide a grant number for this sponsor - University of Adelaide - (if available) and include this number into the main text where appropriate. (p. 14/ line 6)

Please check this box or indicate your approval if you have no corrections to make to the PDF file

Chromium isotope fractionation between modern seawater and biogenic carbonates from the Great Barrier Reef, Australia: Implications for the paleo-seawater δ^{53}Cr reconstruction

Juraj Farkaš [a,b,c], Jiří Frýda [d], Cora Paulukat [e,1], Edmund Hathorne [f], Šarka Matoušková [g], Jan Rohovec [g], Barbora Frýdová [d], Michaela Francová [a], Robert Frei [e]

[a] *Department of Geochemistry, Czech Geological Survey, Prague, Czech Republic*
[b] *Department of Earth Sciences, University of Adelaide, North Terrace, Adelaide, Australia*
[c] *TRaX – Centre for Tectonics, Resources and Exploration, University of Adelaide, North Terrace, Adelaide, SA 5005, Australia*
[d] *Department of Environmental Geosciences, Czech University of Life Sciences, Prague, Czech Republic*
[e] *Department of Geosciences and Natural Resource Management, University of Copenhagen, Denmark*
[f] *GEOMAR, Helmholtz Centre for Ocean Research, Kiel, Germany*
[g] *Institute of Geology, Academy of Sciences of the Czech Republic, Czech Republic*

ABSTRACT

This study investigates chromium isotope variations (δ^{53}Cr) and REE patterns in present-day biogenic carbonates and ocean waters from Lady Elliot Island (LEI) located in the southern Great Barrier Reef (GBR), Australia, which is one of the world's largest carbonate-producing shelf ecosystems. Our results from thoroughly cleaned biogenic carbonates collected at LEI, with no detectable evidence for lithogenic Cr and/or Mn–Fe oxide coating contamination, revealed a systematic and statistically significant correlation ($r^2 = 0.83$, $p < 0.05$) between δ^{53}Cr and cerium anomaly (Ce/Ce*) data in molluscan shells (i.e., gastropods). This in turn implies a redox-controlled incorporation of Cr from seawater into a shell during mineralization mediated by the organism. In particular, shells with higher δ^{53}Cr values, which approach the Cr isotope composition of local seawater, tend to be associated with more negative Ce/Ce*. Importantly, the intercept of the above δ^{53}Cr vs. Ce/Ce* correlation points to the Cr isotope composition of local ocean water, which has an average δ^{53}Cr of $+0.82\pm0.13$‰ (2σ, relative to SRM 979). These findings thus indicate that the above multi-proxy approach could be used to reconstruct the δ^{53}Cr signature of local paleo-seawater based on Ce/Ce* and δ^{53}Cr data in a set of well-preserved fossil skeletal carbonates (i.e., molluscan shells) collected at a specific site. Interestingly, the only calcifying organism from LEI that yielded identical δ^{53}Cr vs. Ce/Ce* values as those in ambient ocean water was a microbial calcitic carbonate produced by red coralline algae (*Lithothamnion* sp.). This organism thus seems to incorporate Cr isotopes and REE from seawater without additional biological discrimination and/or isotope fractionation effects. Considering that calcite is a more stable CaCO$_3$ polymorph during post-depositional alternation and diagenetic stabilization of marine carbonates (compared to aragonite), the fossil counterparts of these algal-microbial carbonates (microbialites) might thus represent ideal natural archives of the paleo-seawater δ^{53}Cr and Ce/Ce* variations over geological time.

Finally, our compilation of δ^{53}Cr data from recent marine biogenic carbonates originating from the main oceanic provinces (South/North Pacific, South/North Atlantic, Caribbean, Mediterranean Sea) confirms that marine carbonates tend to be systematically enriched in light Cr isotopes relative to local ocean waters. Trace element constraints, however, indicate that some of these shifts to lower δ^{53}Cr values (i.e., approaching -0.1 per mil) are related to a presence of lithogenic Cr in the shells, causing a diagenetic overprint of the primary marine δ^{53}Cr signal.

© 2018 Elsevier B.V. All rights reserved.

1. Introduction

Chromium (Cr) is a redox-sensitive transition metal with four naturally occurring isotopes (^{50}Cr, ^{52}Cr, ^{53}Cr and ^{54}Cr) that could

be used as tracers to constrain present and past redox conditions on Earth and other solar system objects (Bonnand et al., 2016; Schoenberg et al., 2016; Crowe et al., 2013; Planavsky et al., 2014; Frei et al., 2009). Stable Cr isotopes can also be utilized to monitor the sources and biogeochemical pathways of chromium within terrestrial reservoirs including geological, hydrological and biological systems (Paulukat et al., 2016; Holmden et al., 2016; D'Arcy et al., 2016; Wang et al., 2016; Pereira et al., 2015; Scheiderich et al., 2015; Farkaš et al., 2013; Bonnand et al., 2013; Schoenberg et al., 2008; Ellis et al., 2002). Although Cr can occur in numerous oxidation states (ranging from -2 to $+6$; cf., Daulton and Little, 2006), in most near-surface terrestrial environments including the oceans, it is typically present either as trivalent Cr(III) or hexavalent Cr(VI) species, depending on local redox conditions (Kotaś and Stasicka, 2000; Elderfield, 1970; Pettine and Millero, 1990).

Importantly, there is a systematic fractionation of stable Cr isotopes (i.e., $^{53}Cr/^{52}Cr$ ratios or $\delta^{53}Cr$) in nature due to redox processes, where the reduction of Cr in near-surface environments produces dissolved Cr(VI) that is isotopically heavier, relative to a less soluble Cr(III) species (Ellis et al., 2002; Zink et al., 2010; Døssing et al., 2011). The Cr isotope composition of seawater thus reflects a complex signal of oxidation/reduction processes operating within the oceans (Scheiderich et al., 2015; Paulukat et al., 2016), and the $\delta^{53}Cr$ record of marine sedimentary archives has potential to be used to infer the past redox conditions of the ocean–atmosphere system through geological time (Frei et al., 2009, 2011, 2013, 2016; Bonnand et al., 2013; Van Zuilen and Schoenberg, 2013; Planavsky et al., 2014; Holmden et al., 2016; D'Arcy et al., 2016; Rodler et al., 2016; Gilleaudeau et al., 2016).

Due to a basically continuous geological record of marine carbonates throughout most of the Earth's history, i.e., the last $\sim$3.7 billion years (Nutman et al., 2016; Shields and Veizer, 2002), Cr isotope studies of marine carbonate archives are particularly appealing for paleo-redox reconstructions. However, as shown by recent studies (Rodler et al., 2015; Pereira et al., 2015; Wang et al., 2016), the actual mechanism(s) of Cr incorporation and redox-controlled isotope fractionation during the formation of inorganic and biogenic carbonates is rather complex and poorly understood, thus requiring further systematic investigations in both natural and laboratory-controlled settings. Available results from inorganic calcite precipitation experiments have revealed that the incorporation of Cr from a solution into $CaCO_3$ is facilitated as chromate anion (CrO_4^{2-}), which replaces carbonate anion (CO_3^{2-}) in the calcite lattice (Tang et al., 2007). This process of inorganic calcification tends to preferentially incorporate heavy ^{53}Cr isotopes into the mineral, yielding a $\delta^{53}Cr$ of calcite which is thus up to $\sim$0.3‰ more positive compared to the fluid (Rodler et al., 2015). In contrast, biologically produced marine $CaCO_3$ minerals, such as foraminiferal calcite (Wang et al., 2016), coral aragonite (Pereira et al., 2015) and bulk carbonate sediments (Holmden et al., 2016), are all systematically enriched in light Cr isotopes compared to ambient seawater. This fractionation trend is thus the exact opposite of the situation observed in inorganic calcite (cf., Rodler et al., 2015).

Furthermore, due to local redox cycling and biological uptake of Cr in the oceans (Semeniuk et al., 2016), the Cr isotope signature of present-day seawater is not globally homogeneous (Scheiderich et al., 2015; Paulukat et al., 2016), further complicating the application of the $\delta^{53}Cr$ proxy in marine carbonate archives. Considering the abovementioned issues and limitations, the full potential of Cr isotopes for paleo-redox studies can only be realized with more detailed calibration work done on the modern seawater-carbonate system from different oceanographic settings, by analyzing $\delta^{53}Cr$ data from both local seawater and precipitated marine carbonates.

This study is the first to present such a comprehensive Cr isotope investigation of the seawater-carbonate system from one of the world's largest carbonate-producing shelf ecosystems, the Great Barrier Reef (Lady Elliot Island, Australia), where $\delta^{53}Cr$ data were acquired from local ocean waters and selected recent biogenic carbonates (i.e., gastropods, cephalopods, corals, and calcifying algae). In addition, an alternative and complementary redox proxy, i.e., Cerium anomaly (Ce/Ce*), is applied here to further test and quantify the possible role of redox processes during Cr incorporation into marine biogenic carbonates. Elemental abundances of selected elements (Al, Mn, Fe, and REE), coupled with $^{87}Sr/^{86}Sr$ analysis, are also used as indices to evaluate possible contamination by non-marine Cr sources originating from lithogenic (detrital minerals, clays) and/or Mn–Fe oxide components (Pereira et al., 2015; Wang et al., 2016; Rodler et al., 2016; Gilleaudeau et al., 2016). The Cr isotope data acquired from the seawater-carbonate system at Lady Elliot Island are complemented by additional $\delta^{53}Cr$ analyses of marine skeletal carbonates (i.e., bivalves, gastropods) collected from the main oceanic provinces including: North and South Atlantic, North and South Pacific Oceans, and the Mediterranean Sea. Finally, these are then compared to published seawater $\delta^{53}Cr$ signatures for the above oceanic provinces (Scheiderich et al., 2015; Paulukat et al., 2016), and conclusions are made about the redox-controlled mechanism(s) behind the Cr isotope fractionation in a seawater-carbonate system, with implications for paleo-seawater $\delta^{53}Cr$ reconstructions.

2. Study sites and samples

Lady Elliot Island ($24°06'47''S$, $152°44'50''E$) is the southernmost tropical coral cay of the Great Barrier Reef (GBR), which is the largest coral reef ecosystem on Earth with in-situ production of skeletal carbonates within an area comprising about 344,400 km², stretching along $\sim$2300 km off the coastline of Queensland, Australia (Fig. 1), (De'ath et al., 2012; Chivas et al., 1986). Lady Elliot Island (LEI) represents a particularly interesting and unique site for Cr isotope studies mostly because of (i) its remote location from the Australian mainland (ca. 80 km from the nearest coastline), and (ii) the effect of prevailing south-easterly trade winds blowing from the open ocean towards the mainland (Kench and Brander, 2006). Together these presumably result in a minimum input of possible continentally-derived Cr sources (i.e., mineral dust, silicate detritus) into the studied seawater-carbonate system. This unique setting of LEI, in turn, minimizes potential contamination of our samples with lithogenic/detrital Cr, which has been proven to impact $\delta^{53}Cr$ measurements in naturally Cr-poor marine carbonates (Pereira et al., 2015; Wang et al., 2016; Rodler et al., 2016).

The reef platform of LEI is kidney-shaped, measuring $\sim$1.2 km along its longest (NE-SW) and $\sim$0.8 km along its shorter (SE-NW) axis, with typical water depths ranging from <1 to about 25 m, across the reef-flat and reef-slope areas, respectively (Hamylton, 2014). Seawater samples analyzed in this study (Fig. 1C) were collected in 2015 by the LEI's Eco Resort scuba-diving team on (i) the leeward side of the island from the reef-flat and slope areas (near Coral Garden), and also on (ii) the windward side from the northeast lagoon (i.e., a reef-flat) and the northerly surf-break area (i.e., near a reef slope), (see also Table 1).

The main shallow-water calcifying organisms and benthic carbonate producers at the LEI's reef platform are: (i) scleractinian corals, (ii) red coralline algae, (iii) green calcifying algea (*Halimeda*), and marginally also (vi) benthic foraminifera, bivalves, and gastropods (Hamylton, 2014). Samples of recent biogenic carbonates were collected in 2013 from the leeward side of LEI, in an area called the 'Coral Gardens' (Fig. 1), and these specimens were sampled under the Queensland Museum general purposes permit.

Table 1

Ocean waters from Lady Elliot Island (LEI), the Great Barrier Reef, South Pacific Ocean (background data, chromium concentrations and isotope compositions).

Sample ID	Material	Coordinates: latitude/longitude	Sampling site: other specifications	Depth (m)	Cr (ng/kg)	δ^{53}Cr (‰)	2sd	*n*
SW 1	Seawater	24°06′35″S, 152°42′48″E	Leeward side/Reef flat	~0.5	193	0.75	0.03	1
SW 2	Seawater	24°06′31″S, 152°42′42″E	Leeward side/Reef slope	~0.5	191	0.80	0.01	2
SW 3	Seawater	24°06′30″S, 152°42′58″E	Windward side/Reef flat	~0.5	202	0.72	0.10	2
SW 4	Seawater	24°06′19″S, 152°42′56″E	Windward side/Reef slope	~0.5	173	1.01	0.08	2
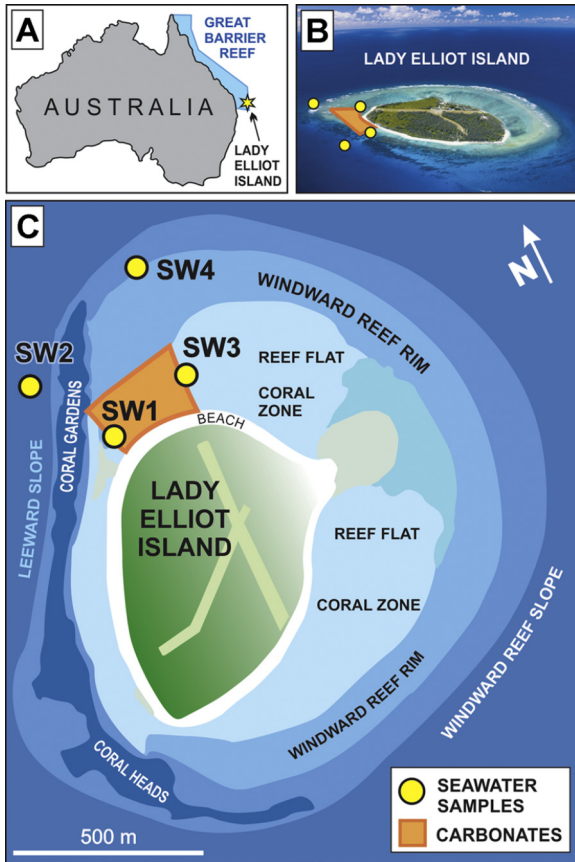
Fig. 1. (**A**) Map showing the study site, i.e., Lady Elliot Island (LEI), located in the southern Great Barrier Reef (GBR), Australia. (**B**) An aerial view of LEI with indicated sampling sites for ocean waters (yellow circles) and marine biogenic carbonates (orange polygon). (**C**) Schematic map of the island showing different zones within the LEI's reef system (i.e., flat, rim, slope), also including the sampling locations for seawaters and marine carbonates. (For interpretation of the colors in the figure(s), the reader is referred to the web version of this article.)

Importantly, the studied biogenic carbonates from LEI contain all the major representatives of key carbonate producing organisms including: (i) scleractinian corals, (ii) calcifying algae, (iii) and numerous species of gastropods (Table 2; and Fig. A1 and Table A1, Appendix).

To explore the range of δ^{53}Cr values, and their relationships to REE patterns in marine skeletal carbonates on a global scale, we also assembled and analyzed different species of recent bivalves and gastropods collected from numerous locations worldwide, i.e. other locations (OL), which represent the main oceanic provinces including: North and South Atlantic, North and South Pacific Oceans, and the Mediterranean Sea (Table 3; Fig. A2 and Table A2, Appendix).

3. Methods

3.1. Sample preparation

Seawater samples from LEI were collected into pre-cleaned plastic bottles and stored in a fridge until elemental and isotope analyses. Prior to analysis the samples were filtered through 0.45 μm nylon membrane filters (Advantec MFS) and acidified.

Biogenic carbonates used for the isotope and elemental analysis were first physically scarped and washed in Milli-Q water (MQ, resistivity 18 Mohm/cm), and the shell fragments were then immersed in hydrogen peroxide (H_2O_2) and ethanol (C_2H_6O), followed by a brief leach in 1 N HCl and a final thorough washing in MQ water (following cleaning procedure P-5 from Zaky et al., 2015).

3.2. Elemental concentration analysis (major, trace and REE)

Major and trace element concentrations in biogenic carbonates were analyzed, respectively, by ICP-OES (Agilent 5100) and a sector field ICP-MS Element II (Thermo Fisher Scientific) at the Institute of Geology, Czech Academy of Sciences (for details see Appendix). The REE concentrations in filtered seawater and pre-cleaned LEI carbonates were determined using a seaFAST online pre-concentration system (Elemental Scientific Inc., USA) and ICP-MS (Agilent 7500ce) at GEOMAR. Our methods followed the analytical approach of Hathorne et al. (2012) and Osborne et al. (2017), for seawater and carbonate samples, respectively. Details on analytical errors, reproducibility, detection limits and procedural blanks of the seaFAST REE analyses are available in the Appendix (Tables A3 and A4).

The shale-normalized cerium anomaly (Ce/Ce*) reported in this study is calculated based on the following equation (Webb and Kamber, 2000, and Bau and Dulski, 1996):

$$Ce/Ce^*$$
$$= [Ce/Ce_{(PAAS)}]/[0.5 \times (La/La_{(PAAS)}) + 0.5 \times (Pr/Pr_{(PAAS)})] \quad (1)$$

where PAAS represents the 'Post-Archean Average Australian Shale' (cf., Taylor and McClennan, 1985).

3.3. Strontium isotope analysis (^{87}Sr/^{86}Sr) by TIMS

Selected samples of biogenic carbonates and seawaters (both filtered and unfiltered) from LEI were analyzed for ^{87}Sr/^{86}Sr ratios by TIMS (VG Sector 54 IT) at the University of Copenhagen. Briefly, Sr was purified from samples using SrSpec resin, and eluted Sr was loaded on single Re filaments with a Ta_2O_5–H_3PO_4–HF activator. The presented ^{87}Sr/^{86}Sr values were corrected for the offset relative to the certified NIST SRM 987 of 0.710248 (McArthur et al., 2006). The reported errors (2σ) are within-run precisions of the individual analysis.

Table 2

Marine biogenic carbonates from Lady Elliot Island (LEI), the Great Barrier Reef, South Pacific Ocean (background data, mineralogy, elemental and isotope compositions).

Sample ID	Carbonate mineralogy	Coordinates: latitude/longitude	Organism order/phylum	Cr (ppm)	δ^{53}Cr (‰)	2sd	n	Al (ppm)	Fe (ppm)	Mn (ppm)	D_{Cr} (c/sw)
LEI 1	Aragonite	24°06′33″S 152°42′56″E	*Vetigastropoda* Mollusca	0.042	0.31	0.08	2	5.0	11.2	1.1	221
LEI 2	Aragonite	24°06′33″S 152°42′56″E	*Scleractinia* Cnidaria – Coral	0.148	0.40	0.06	3	34.7	47.6	1.7	779
LEI 3	Aragonite	24°06′33″S 152°42′56″E	*Scleractinia* Cnidaria – Coral	0.096	0.32	0.06	7	15.3	55.8	0.9	505
LEI 4	Aragonite	24°06′33″S 152°42′56″E	*Sepiida* Mollusca	0.076	0.34	0.07	4	10.5	30.7	1.8	400
LEI 5	Aragonite	24°06′33″S 152°42′56″E	*Caenogastrop.* Mollusca	0.072	0.61	0.05	3	6.3	8.3	0.8	379
LEI 6	Aragonite	24°06′33″S 152°42′56″E	*Vetigastropoda* Mollusca	0.034	0.35	0.08	2	4.8	23.2	1.1	179
LEI 7	Aragonite + calcite (HMC)	24°06′33″S 152°42′56″E	*Neritimorpha* Mollusca	0.015	0.36	0.09	2	16.3	63.4	3.8	79
LEI 8	Aragonite	24°06′33″S 152°42′56″E	*Caenogastrop.* Mollusca	0.017	0.31	0.09	1	3.1	32.8	2.4	89
LEI 9	Aragonite	24°06′33″S 152°42′56″E	*Vetigastropoda* Mollusca	0.062	0.29	0.07	3	9.8	30.5	0.9	326
LEI 10	Calcite (HMC)	24°06′33″S 152°42′56″E	*Coralline Algae* Rhodophyta	0.450	0.86	0.07	6	10.9	40.7	3.8	2356
LEI 11	Calcite (HMC)	24°06′33″S 152°42′56″E	*Alcyonacea* Cnidaria – Coral	2.081	0.42	0.06	7	58.4	61.4	3.0	10895
LEI 12	Aragonite + calcite (HMC)	24°06′33″S 152°42′56″E	*Coralline Algae* Rhodophyta	0.191	0.45	0.07	6	10.5	21.1	1.6	1000

3.4. Chromium isotope analysis ($\delta^{53/52}$Cr) by TIMS

The acid-digested samples (i.e., filtered seawaters and pre-cleaned carbonates) were spiked with ^{50}Cr–^{54}Cr tracer (i.e., double spike) and processed through a two-step Cr purification chromatography, using a combination of anionic and cationic exchange columns. Purified Cr fractions were analyzed on an IsotopX Phoenix thermal ionization mass spectrometer (TIMS) at the University of Copenhagen (Frei et al., 2009; Pereira et al., 2015). The Cr isotope composition of a sample is expressed as δ^{53}Cr notation (normalized to SRM 979) in per mil (‰), according to the following equation:

$$\delta^{53}\text{Cr (‰)}$$
$$= \left[\left(^{53}\text{Cr}/^{52}\text{Cr}\right)_{\text{SAMPLE}} / \left(^{53}\text{Cr}/^{52}\text{Cr}\right)_{\text{SRM979}} - 1 \right] \times 1000 \qquad (2)$$

The external reproducibility of the δ^{53}Cr data is about ± 0.05‰ (2sd), based on repeated measurements of certified standards (SRM 979, JDo-1 and JLs-1) and samples (Tables 2 and 3).

4. Results

4.1. Oceanic waters – chromium isotope compositions (δ^{53}Cr) and elemental concentrations

A total of 4 seawater samples (i.e., South Pacific ocean waters) collected at different sites in the vicinity of Lady Elliot Island (Fig. 1C) were analyzed for δ^{53}Cr, Cr and REE concentrations (see data in Table 1; and Table A5, Appendix). The Cr concentrations of LEI seawater range from 173 to 202 ng/kg, and their δ^{53}Cr spread from ~0.72‰ to ~1.01 $\pm$ 0.05‰ (Fig. 2A), thus overlapping with published data for 'global surface ocean' waters collected from other locations (Paulukat et al., 2016; Scheiderich et al., 2015). Importantly, our results reveal a strong and statistically significant correlation ($r^2 = 0.96$, $p < 0.05$) between δ^{53}Cr and concentration [Cr] data in LEI seawaters (Fig. 2B, C). Such coupling between

Cr isotope compositions and concentrations has also been observed in ocean waters collected worldwide (Paulukat et al., 2016; Scheiderich et al., 2015). But the latter global dataset yields a specific slope of -0.79 which thus differs from that of the LEI's seawaters. The latter yield a slope of -1.93 ± 0.27 (1σ) in a cross-plot with δ^{53}Cr vs. ln[Cr] coordinates (Fig. 2C). The REE analysis of LEI seawaters (with the exception of a sample SW 1) show patterns typical for coastal seawater from the Great Barrier Reef, with characteristic enrichments of heavy REE and generally less negative Ce/Ce* anomalies ranging from ~0.322 to ~0.592 (i.e., data from this study and Wyndham et al., 2004), compared to typical seawater from the Pacific Ocean with a more pronounced negative Ce/Ce* anomaly of ~0.054 (see data in Tables A7 and A8, Appendix).

### 4.2. Biogenic carbonates – chromium isotope variations (δ^{53}Cr) and elemental concentrations

A total of 29 recent marine biogenic carbonates were analyzed for δ^{53}Cr values and elemental concentrations (i.e., Cr, Mg, Sr, Al, Fe, Mn, and REE), including 12 samples from LEI (Table 2), and 17 skeletal carbonates originating from 'other locations' (OL) worldwide. For details see also the Appendix and elemental data for LEI and OL samples listed in Tables A5 and A6, respectively (REE data are in Tables A9 and A10).

Overall, the investigated biogenic carbonates ($n = 29$) yielded Cr concentrations ranging from ~0.008 to ~2.081 ppm, and their δ^{53}Cr values range from ~0.05‰ to ~0.86 $\pm$ 0.07‰, with no statistically significant correlation between δ^{53}Cr and Cr concentration data ($r^2 = 0.29$, $p = 0.12$). Nevertheless, there is an apparent systematic difference between δ^{53}Cr signatures of carbonates from LEI, and those from OL ($p < 0.0001$). The former yields an average δ^{53}Cr of ~0.42 $\pm$ 0.16‰ (1sd, $n = 12$), whereas the latter sample set gives a much lower average of ~0.14 $\pm$ 0.12‰ (1sd, $n = 17$) (Tables 2 and 3). There seems to be no obvious correlation between δ^{53}Cr signatures and Al or Fe concentrations (or Al/Cr and Fe/Cr elemental ratios) of the investigated carbonates

Table 3

Marine biogenic carbonates from other locations (OL) worldwide, including Mediterranean Sea, North and South Atlantic, and North Pacific Ocean (background data, elemental and isotope compositions).

Sample ID	Oceanic/sea water body	Location country	Coordinates: latitude/longitude	Organism class/phylum	Cr (ppm)	δ^{53}Cr (‰)	2sd	n	Al (ppm)	Fe (ppm)	Mn (ppm)
OL 1	Mediterranean	*Italy* Sicily	37°59′43″N 13°40′30″E	*Bivalvia* Mollusca	0.041	0.20	0.09	4	1.5	4.3	2.1
OL 2	Mediterranean	*Italy* Sicily	37°59′43″N 13°40′30″E	*Gastropoda* Mollusca	0.059	0.16	0.06	4	3.6	2.8	3.7
OL 3	Mediterranean	*Italy* Bellaria	44°07′56″N 12°29′16″E	*Gastropoda* Mollusca	0.180	0.08	0.06	9	8.6	9.5	27.6
OL 4	Mediterranean	*Italy* Bellaria	44°07′56″N 12°29′16″E	*Bivalvia* Mollusca	0.510	0.05	0.10	9	15.4	20.7	35.0
OL 5	Mediterranean	*Italy* Bellaria	44°07′56″N 12°29′16″E	*Bivalvia* Mollusca	0.047	0.10	0.08	7	1.8	12.1	10.7
OL 6	North Atlantic	*Brittany* Carnac	47°34′14″N 03°04′31″W	*Gastropoda* Mollusca	0.098	0.19	0.07	6	2.1	28.0	6.8
OL 7	North Atlantic	*Brittany* Carnac	47°34′14″N 03°04′31″W	*Gastropoda* Mollusca	0.008	0.06	0.20	1	1.3	0.9	1.5
OL 8	North Atlantic	*Brittany* Brest	48°17′33″N 04°27′14″W	*Gastropoda* Mollusca	0.085	0.12	0.06	7	4.6	53.4	0.7
OL 9	North Atlantic	*Brittany* Carnac	47°34′14″N 03°04′31″W	*Bivalvia* Mollusca	0.015	0.08	0.09	1	1.7	22.5	1.9
OL 10	North Atlantic	*Norway* Oslo	59°19′36″N 10°40′06″E	*Bivalvia* Mollusca	0.053	−0.02	0.06	3	3.1	35.1	4.0
OL 11	South Atlantic	*Argentina* Viedma	41°09′20″S 63°07′49″W	*Gastropoda* Mollusca	0.064	0.20	0.08	4	33.1	152.4	3.1
OL 12	South Atlantic	*Argentina* Viedma	41°09′20″S 63°07′49″W	*Bivalvia* Mollusca	0.025	0.14	0.08	1	1.9	3.1	23.5
OL 13	South Atlantic	*Argentina* Viedma	41°09′20″S 63°07′49″W	*Gastropoda* Mollusca	0.043	0.25	0.11	3	3.6	3.6	1.6
OL 14	North Pacific	*USA* Alaska	56°50′37″N 134°00′24″W	*Gastropoda* Mollusca	0.017	0.10	0.09	2	0.6	3.4	0.6
OL 15	North Pacific	*USA* Alaska	56°50′37″N 134°00′24″W	*Bivalvia* Mollusca	0.272	0.54	0.07	12	0.3	23.9	0.1
OL 16	North Pacific	*USA* Alaska	56°50′37″N 134°00′24″W	*Bivalvia* Mollusca	0.048	0.11	0.06	6	2.3	49.0	0.5
OL 17	North Pacific	*USA* Oregon	44°29′11″N 124°05′05″W	*Gastropoda* Mollusca	0.130	0.07	0.07	7	15.9	15.1	3.3
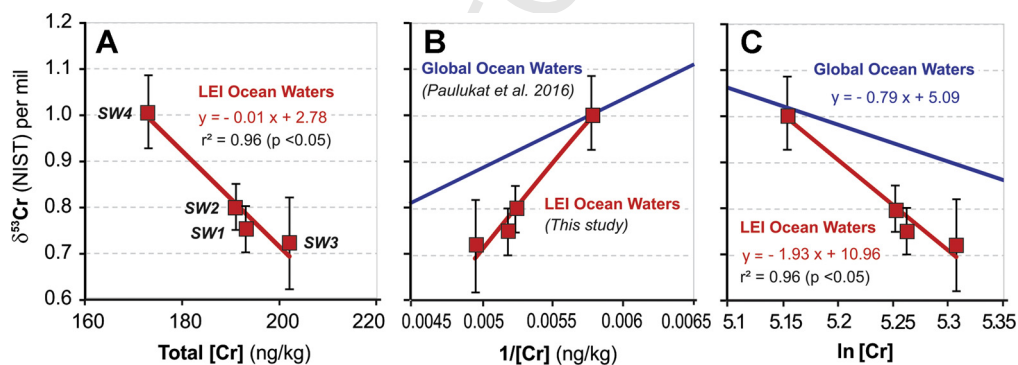
**Fig. 2.** (**A**) The Cr isotope compositions (δ^{53}Cr) and concentrations (ng/kg) in ocean waters collected from Lady Elliot Island (LEI), with a linear regression trend (i.e., red line) fitted to seawater data. (**B**) δ^{53}Cr versus 1/[Cr] with logarithmic trends through data, where the red line represents a log fit function for LEI seawater samples, and the blue trend was constructed using the 'global seawater dataset' compiled by Paulukat et al. (2016); see also references therein. (**C**) δ^{53}Cr versus ln[Cr] cross-plot with linear regression trends: red line = LEI data; and blue line = Global Ocean Water dataset from Paulukat et al. (2016).

from LEI and OL (Fig. A4), which might suggest a lack of contamination from detrital clays and/or Fe-oxides (Wang et al., 2016; Pereira et al., 2015). However, a cross-plot of Cr isotopes versus Mn/Cr ratios (Fig. A5) reveals that biogenic carbonates from OL yield systematically lower δ^{53}Cr and relatively higher Mn/Cr, compared to samples from LEI. This difference was also confirmed by the non-parametric Mann–Whitney U statistic test (an equivalent for the parametric Student t-test; for details see the Appendix). This, in turn, points to a possible contamination issue related to Mn-oxide coatings on the measured Cr isotope compositions of

carbonates collected from other locations (OL), which are indeed expected to be more impacted by terrestrial inputs and lithogenic Cr sources (due to their proximity to continents) relative to samples from LEI.

As for REE, the samples from LEI exhibit rather low ΣREE ranging from ~1.5 to 93 (ppb), and variable true negative Ce/Ce* (PAAS) anomalies from ~0.298 up to ~0.825 (Table A9), whose fidelity was confirmed also via Ce/Ce* vs. Pr/Pr* and La/Ce cross-plots (see Fig. A3, Appendix). A very similar range was observed in the samples from OL, which yielded Ce/Ce* from ~0.375 to ~0.925, but
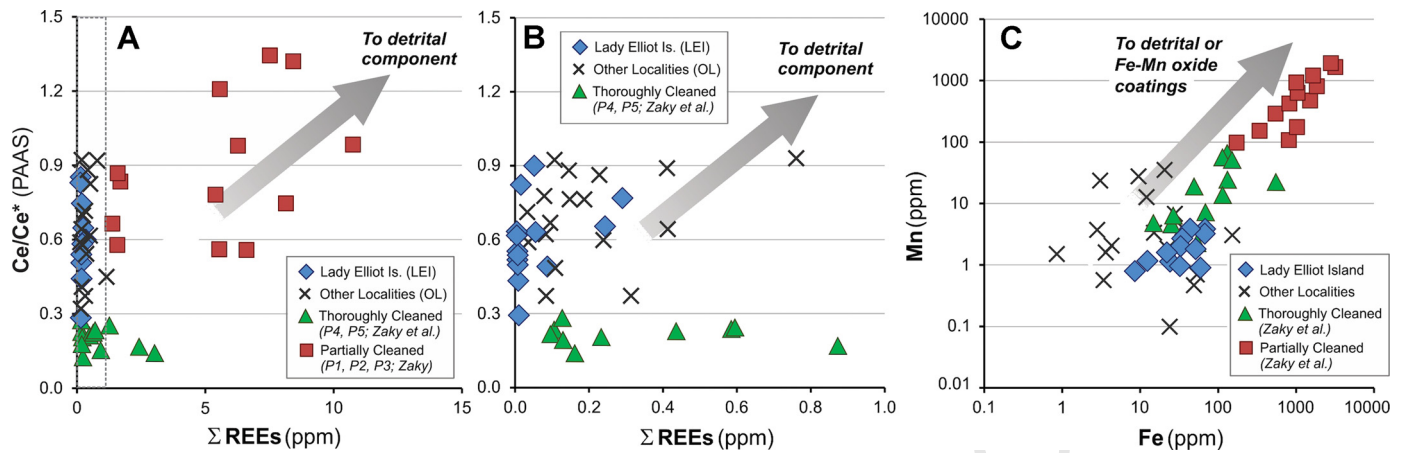
Fig. 3. (**A**) Ce/Ce* and ΣREE for pre-cleaned LEI and OL biogenic carbonates (this study), and datasets from different cleaning procedures performed on modern biogenic carbonates (i.e., brachiopod shells) by Zaky et al. (2015). The latter study includes 'thoroughly cleaned' samples (i.e., P4 and P5 datasets) that involved a combination of physical and chemical cleaning (i.e., scraping, sonication in Milli-Q water and H_2O_2, and leaching in HCl acid); and 'partially cleaned' samples that only went through physical cleaning and/or H_2O/H_2O_2 washing (i.e., P1, P2 and P3 datasets; for details see Zaky et al., 2015). (**B**) A close-up view of the datasets presented in Fig. 3A (see the dashed rectangle). (**C**) A cross-plot of Mn vs. Fe concentrations (ppm) in LEI and OL biogenic carbonates, and datasets from different cleaning procedures of Zaky et al. (2015).

their ΣREE are systematically higher, i.e., ranging from $\sim$37 up to 998 (ppb), (Table A10). Interestingly, the biogenic carbonates from LEI (i.e., benthic molluscs) reveal a strong and statistically significant negative correlation ($r^2 = 0.83$, $p < 0.05$, $n = 6$) between δ^{53}Cr and Ce/Ce*, the latter being a redox proxy. A very similar relationship between Cr isotopes and Ce/Ce* anomaly data was observed recently by Bonnand et al. (2013) in modern marine ooids from the Bahamas ($r^2 = 0.93$, $p < 0.05$, $n = 4$). However, no such correlation between δ^{53}Cr and Ce/Ce* was observed in our samples of corals and calcareous algae from LEI, nor in our data from the OL samples (see Appendix, Fig. A6).

4.3. Strontium isotopes (^{87}Sr/^{86}Sr) in seawaters and biogenic carbonates from LEI

Seawater collected from LEI (filtered and unfiltered) yielded ^{87}Sr/^{86}Sr ratios ranging from 0.709162 to 0.709171, with a mean of 0.709166 $\pm$ 0.000005 (2σ, $n = 10$; Table A12, Appendix), which is consistent with present-day global ocean water (McArthur et al., 2006; Pereira et al., 2015). As for biogenic carbonates from LEI (Table A13), their ^{87}Sr/^{86}Sr ranges from 0.709161 to 0.709175, giving a mean of 0.709168 $\pm$ 0.000008 (2σ, $n = 24$), which thus overlaps within error with the mean ^{87}Sr/^{86}Sr of LEI seawater (Fig. 4).

5. Discussion

5.1. Evaluating the effect of contamination by detrital/lithogenic components and Mn/Fe oxide coatings via ΣREE, trace elements and ^{87}Sr/^{86}Sr indices

Numerous studies have shown that adsorbed detritus and/or oxide coatings on marine biogenic carbonates may lead to (i) elevated ΣREE concentrations, (ii) positive and non-marine Ce/Ce* values, and/or (iii) increased Mn and Fe concentrations (Zaky et al., 2015, and references therein). To evaluate these effects and their possible impact on the measured Ce/Ce* and Cr isotope variations in the studied biogenic carbonates, we adopted the approach of Zaky et al. (2015) and plot our data in Ce/Ce* vs. ΣREE, and Mn vs. Fe concentration plots (Fig. 3).

For the purposes of comparison, we present our results (i.e., LEI and OL samples) along with data from Zaky et al. (2015) that represent (i) 'thoroughly cleaned' carbonate shells (i.e., physical and chemical treatment = P4 and P5 procedures), and (ii) 'partially cleaned' samples, where the detrital components and oxide coatings were not properly removed (i.e., P1, P2 and P3 procedures).

Importantly, this comparison reveals that our data from LEI and OL carbonates do not show any obvious correlation between Ce/Ce* and ΣREE, where the latter would be indicative of contamination issues. Overall our data plot within the range of ΣREE, Mn and Fe concentrations measured in the 'thoroughly cleaned' samples of Zaky et al. (2015). This in turn points to the effectiveness and suitability of our selected cleaning procedure (i.e. P5, as defined by Zaky et al., 2015).

However, the OL samples exhibit generally higher ΣREE and Mn/Cr ratios, coupled with systematically lower δ^{53}Cr values (compared to the LEI samples; see Fig. 3B, Fig. A5), and these differences between OL and LEI data sets are statistically significant, as confirmed by the Mann–Whitney test (see the Appendix). Such elevated Mn/Cr coupled with low δ^{53}Cr values, the latter approaching -0.1 per mil (i.e., the Cr isotope signature of the Earth's silicate crust; Schoenberg et al., 2008; Farkaš et al., 2013), might thus indicate possible contamination of OL samples by lithogenic Cr sources, possibly related to the presence of Mn-oxide coatings. We speculate that perhaps Mn oxyhydroxides could impact the δ^{53}Cr of marine skeletal carbonates due to oxidation of lithogenic and isotopically light Cr(III) present in local sediments and pore waters to more soluble and mobile Cr(VI) species, and their subsequent incorporation into carbonate shells. The latter could be facilitated either via (i) adsorption of such sediment-derived Cr onto reactive surfaces of oxide coatings or directly onto a shell, or alternatively via (ii) chemical exchange and diffusion of Cr between the shell and local pore fluids at the sediment–seawater interface. These hypothesized pathways can thus explain the generally 'non-marine' and very low Cr isotope signatures observed in the OL samples and their association with elevated Mn concentrations (Fig. A5, Table A6). Note that pore waters are expected to have δ^{53}Cr signatures close to $\sim$0‰ due to a large reservoir of lithogenic Cr hosted in marine sediments that are typically dominated by siliciclastic detrital and/or clay minerals.

Thus, our cleaning procedure seems to be sufficient for the LEI carbonates, which originated from a pristine and remote marine setting with minimum input of detrital and lithogenic Cr sources. This procedure seems, however, to be inadequate for a thorough cleaning and removal of lithogenic Cr from the OL carbonate samples, likely because these have been more exposed and impacted by non-marine Cr sources. Overall, our data seem to indicate that a large part of Cr hosted in the shells from OL might have originated from lithogenic or sediment/pore water derived Cr sources,
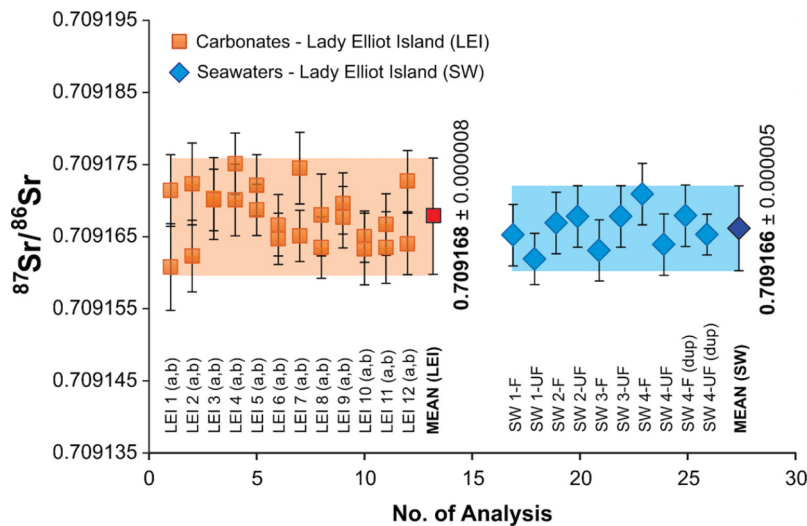
Fig. 4. Strontium isotope ratios (^{87}Sr/^{86}Sr) measured in biogenic carbonates (LEI data) and seawater (SW) collected from Lady Elliot Island. For details see also data listed in Tables A12 and A13. The following abbreviations are used: SW = seawater, F = filtered, UF = unfiltered. Note that for carbonates (i.e., LEI data), two aliquots (a, b) from the same sample were processed via columns and analyzed for ^{87}Sr/^{86}Sr.

which thus overprinted the primary and isotopically heavy marine δ^{53}Cr signal in certain shells.

The above diagenetic interpretation is supported by a single sample of bivalve shell from the OL dataset (i.e., a sample OL 15, from Alaska, North Pacific) that yielded the heaviest Cr isotope composition of +0.54‰, which is thus very close to the expected δ^{53}Cr of ambient seawater (Paulukat et al., 2016). This sample also has the lowest Mn and Al concentrations of all of the OL carbonates analyzed (Tables A6, Figs. A4 and A5). Hence, it seems that apart from this sample, which records a close-to original seawater δ^{53}C signal, the rest of OL shells seem to have their Cr isotope compositions impacted to a variable degree by secondary processes, involving later incorporation of lithogenic Cr mediated by the presence of Mn in the system.

Consequently, our further discussion of Cr isotope variations between seawater and biogenic carbonates is focused primarily on the samples from LEI, which showed minimum or no obvious impact of lithogenic and/or Mn–Fe oxide coating contamination on their measured δ^{53}Cr and Ce/Ce* values. To further corroborate the lack of secondary contamination in the LEI samples, we adopted the approach of Pereira et al. (2015) and also analyzed ^{87}Sr/^{86}Sr in biogenic carbonates and local seawater from the Lady Elliot Island (Tables A12, A13). The above isotope proxy is useful, as shifts to more radiogenic ^{87}Sr/^{86}Sr values in marine carbonates (relative to seawater) would indicate the presence of lithogenic/detrital contamination. Importantly, our data confirmed no detectable radiogenic or non-marine Sr sources in the studied LEI carbonates. As the latter yielded ^{87}Sr/^{86}Sr ratios that are identical (within the analytical error) to the local seawater (see Fig. 4), which in turn is consistent with the global ocean Sr isotope composition. Considering the above constraints from Sr isotopes, as well as Ce/Ce* vs. ΣREE, and Mn vs. Fe concentration plots (Fig. 3, and Fig. A5), we are confident that the geochemical data acquired from the LEI carbonates have not been affected by contamination and early diagenetic processes. This is likely related to the fact that LEI samples originate from a remote carbonate-dominated and detrital-poor marine setting of the Great Barrier Reef, while OL samples are from generally carbonate-poor coastal areas more affected by continental inputs (see Table 3). Therefore, we conclude that δ^{53}Cr and Ce/Ce* values measured in LEI carbonates reflect the primary signal related to redox cycling of Cr and Ce in a local marine environment, and/or micro-environment associated with the biological uptake of these redox-sensitive elements during biocalcification.

5.2. Chromium isotope composition of LEI seawater and the impact of a local redox cycling?

Recent studies have revealed significant heterogeneities with respect to Cr cycling in the oceans, where δ^{53}Cr of seawater ranges from ∼0.2‰ up to ∼1.6‰ as a function of water depth (Scheiderich et al., 2015) and/or geographical location (Paulukat et al., 2016). Importantly, these changes in δ^{53}Cr are tightly coupled to changes in seawater Cr concentrations, following a globally recognized correlation trend (i.e., a linear relationship) with a slope of −0.79 ± 0.06 (Paulukat et al., 2016) when plotted in δ^{53}Cr versus ln[Cr] space (Fig. 2C). Assuming a closed-system Rayleigh fractionation of Cr isotopes in the oceans, the above slope of −0.79 could be interpreted as a common 'global' fractionation factor (ε) associated with the redox cycling of Cr in seawater, specifically with the reduction of Cr(VI) to Cr(III) in the surface oceans and/or oxygen minimum zones (Paulukat et al., 2016; Scheiderich et al., 2015). Accordingly, the fractionation factor (ε) for a closed-system behavior of Cr isotopes can be calculated based on the following relationship (cf., Scheiderich et al., 2015):

$$\Delta^{53}Cr_{SW} = \varepsilon \ln[Cr] \tag{3}$$

where $\varepsilon = 1000 * (\alpha - 1)$ is the fractionation factor in ‰ associated with the reduction of Cr(VI) to Cr(III), and α is the fractionation coefficient; and $\Delta^{53}Cr_{SW}$ is the relative change (i.e., difference) in the δ^{53}Cr signature of dissolved Cr remaining in the seawater. Thus, $\Delta^{53}Cr_{SW}$ versus ln[Cr] should have a slope of ε (Scheiderich et al., 2015).

Consequently, the fractionation factor (ε) associated with the reduction of Cr(VI) to Cr(III) in marine settings can be determined from the logarithmic relationship between Cr concentrations (ln[Cr]) and isotope compositions (δ^{53}Cr) in a suite of seawater samples (Fig. 2C), (Scheiderich et al., 2015; Smith and Kroopnick, 1981).

Interestingly, seawater from LEI also shows a strong coupling between δ^{53}Cr and ln[Cr] data, but with a much steeper slope of −1.93 ± 0.27 (1σ) (Fig. 2C), suggesting significantly larger local isotope fractionation effects during the reduction of Cr(VI) to Cr(III). Alternatively, there could be a locally enhanced input of re-oxidized Cr(VI), originating from the oxidation of isotopically light Cr(III) present in bottom pore waters and/or organically-complexed Cr sources (Paulukat et al., 2016; Semeniuk et al., 2016). With our
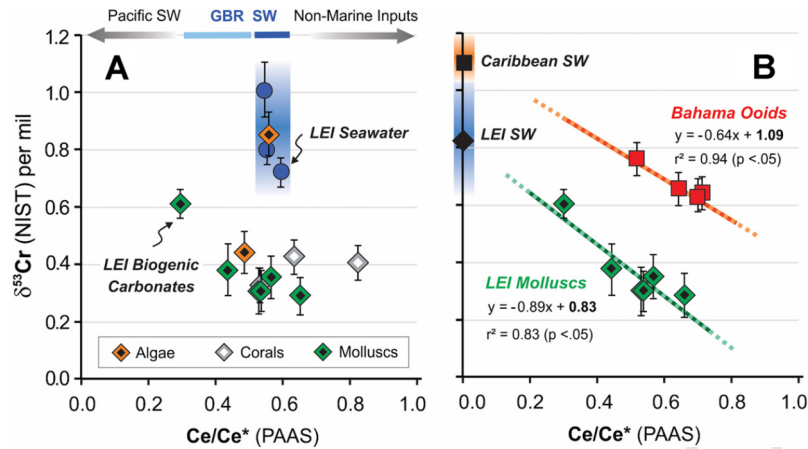
Fig. 5. (**A**) Cr isotope variations (δ^{53}Cr) versus Ce-anomaly data (Ce/Ce*) measured in recent biogenic carbonates (i.e., diamonds) and local seawater (circles) collected from Lady Elliot Island. The following abbreviations are used: LEI = Lady Elliot Island; SW = Seawater; GBR = Great Barrier Reef. The blue vertical rectangle illustrates the range of δ^{53}Cr and Ce/Ce* values measured in LEI seawater (i.e., samples SW 2, 3 and 4); and the light and dark blue horizontal lines illustrates the range of Ce/Ce* anomalies measured in coastal seawaters from the GBR (i.e., data from this study and Wyndham et al., 2004). The grey arrows indicate the directions of negative versus positive Ce/Ce* anomalies, respectively, for Pacific seawater and non-marine (i.e., lithogenic/detrital) continental inputs (see data in Tables A7 and A8, Appendix). (**B**) δ^{53}Cr versus Ce/Ce* data from LEI molluscan shells (i.e., gastropods = green diamonds), and modern ooids from the Great Bahama Bank (i.e., red squares = data from Bonnand et al., 2013). The dashed green and red lines represent linear regression fits constructed for the LEI and Bahama datasets, respectively. Both show a statistically significant ($p < 0.05$) negative correlation between δ^{53}Cr versus Ce/Ce* data. Black diamond represents an intercept value (δ^{53}Cr ≈ +0.83‰) for the LEI's regression trend, which overlaps with the Cr isotope composition of LEI seawater (i.e., blue rectangle) with an average δ^{53}Cr of +0.82 ± 0.13‰. A black square illustrates an intercept for Bahamas ooids data (Bonnand et al., 2013), which overlaps with the δ^{53}Cr of Caribbean seawater (i.e., purple rectangle) with an average of +1.13‰ (Holmden et al., 2016). Note that the presented correlation coefficients (r^2) and p-values are calculated for standard parametric tests (i.e., Pearson correlation), but even if evaluated by non-parametric tests (i.e. Kendall's tau correlation analysis) the p-value for LEI data is still ∼0.05, thus confirming the statistical significance of the observed δ^{53}Cr versus Ce/Ce* correlation trend.

limited dataset, we cannot differentiate between the above scenarios (i.e., a local mixing versus Rayleigh). Future detailed studies of the Cr isotope cycling in shallow-water reef environments could help to better understand these local redox processes, their controlling factors, and effects on the Cr isotope composition of seawater (for details see also the discussion in Appendix).

5.3. Evidence for redox-controlled incorporation of Cr into marine biogenic carbonates

5.3.1. Lady Elliot Island – chromium isotopes (δ^{53}Cr) versus Cerium anomalies (Ce/Ce*)

To further investigate a possible role of biologically mediated redox processes during the incorporation of Cr from seawater and/or a calcifying fluid into biogenic carbonate, we investigated the relationship between δ^{53}Cr and Ce/Ce* data in our samples, as the latter proxy represents a sensitive redox indicator in marine settings (de Baar et al., 1985; Zaky et al., 2015). Briefly, under reducing marine conditions (i.e., anoxic and suboxic settings), Ce in seawater will be present mostly as soluble Ce(III) species, but in oxidizing environments the removal of Ce via uptake by Mn-oxides and its subsequent precipitation as insoluble Ce(IV) will be promoted (Elderfield, 1988; German and Elderfield, 1990). Due to the above redox-controlled partitioning of Ce in seawater, the oxidative removal of Ce from a solution can be quantified via measured Ce abundances normalized to the rest of REE concentration data (i.e., Ce/Ce* anomaly, see Eq. (1); Bau and Dulski, 1996; Webb and Kamber, 2000). In addition, biological processes such as the microbial oxidation of Ce in marine environments play also an important role in controlling the local redox cycling of Ce in seawater, and/or calcification fluids from which marine carbonates precipitate (Moffett, 1990; Wyndham et al., 2004).

Interestingly, our results from LEI biogenic carbonates, specifically benthic molluscan shells (i.e., gastropods), reveal a strong and statistically significant negative correlation between Ce/Ce* and δ^{53}Cr data ($r^2 = 0.83$, $p = 0.01$, $n = 6$; see Fig. 5A, B). In particular, shells with heavier Cr isotope compositions (approaching the δ^{53}Cr of local seawater) yield more negative Ce anomalies (Ce/Ce* ∼ 0.3) which in turn suggest relatively more oxic conditions, or oxidizing

micro-environment, at the site of calcification during the biological uptake of Ce and Cr from seawater (Fig. 5A). Alternatively, the observed coupling between Ce/Ce* and δ^{53}Cr data in shells could also perhaps be related to specific biological activity and ontogenesis of an organism, causing a preferential uptake of Ce and light Cr isotopes into organic matter (or the expulsion from a calcifying fluid), leaving the composition of a shell with lower Ce/Ce* and higher δ^{53}Cr.

It should be pointed out, however, that a very similar negative correlation between Ce/Ce* and δ^{53}Cr data ($r^2 = 0.94$, $p = 0.03$, $n = 4$), with a similar slope, was also documented recently for modern non-skeletal (microbial) marine carbonates, i.e., ooids, from the Bahama Bank (Fig. 5B; data from Bonnand et al., 2013). Importantly, for both of these relationships (i.e., our shells and published ooids) the intercepts of Ce/Ce* versus δ^{53}Cr correlation overlap with the measured Cr isotope composition of local ocean waters (Fig. 5B). Specifically, the intercept for LEI shells is +0.83 ± 0.10 (1σ), and local LEI seawater yielded an average δ^{53}Cr of +0.82 ± 0.13‰ (σ, $n = 4$), (see data in Table 1). As for Bahamas samples, the intercept for ooids is +1.09, while the published data for Caribbean seawaters have an average δ^{53}Cr of +1.14 ± 0.03‰ (σ, $n = 3$), (Holmden et al., 2016).

These purported agreements between δ^{53}Cr of local seawaters and intercepts derived from Ce/Ce* vs. δ^{53}Cr relationships (Fig. 5) perhaps suggest that marine biogenic carbonates that precipitated under more oxidizing conditions or micro-environments (i.e., yielding the most negative Ce anomaly) might actually reflect the Cr isotope signature, approaching the composition of ambient ocean water. The latter might then be inferred from the intercept of Ce/Ce* vs. δ^{53}Cr correlation acquired from a set of suitable marine carbonate archives (e.g., molluscan shells and/or microbial ooids). If validated by future studies, this approach could be used to reconstruct the δ^{53}Cr signature of paleo-seawater based on Ce/Ce* and δ^{53}Cr data in a set of well-preserved fossil marine carbonates collected at a specific site.

Interestingly, the only calcifying organism from the LEI location that yielded identical δ^{53}Cr and Ce/Ce* values to those measured in ambient ocean water was a microbial carbonate (i.e., high-
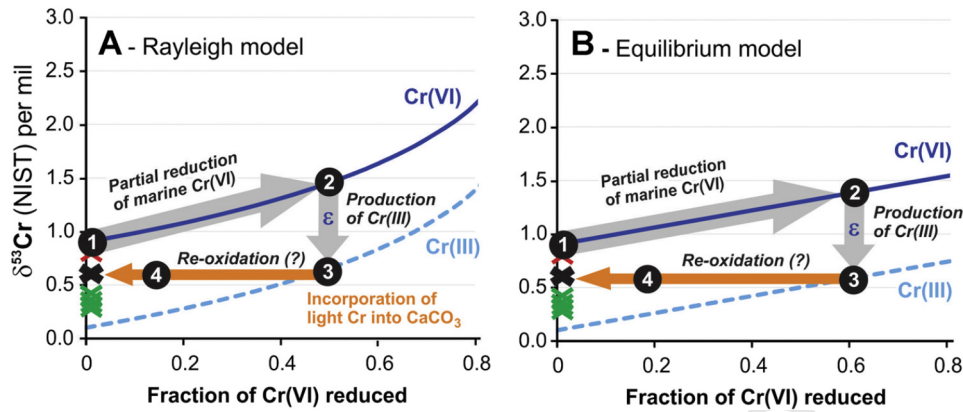
Fig. 6. Conceptual models for the isotope fractionation and redox cycling of Cr during biological uptake and calcification by marine organisms. (**A**) *Rayleigh model* with a finite reservoir of unreacted Cr(VI) pool in calcifying fluids, which does not interact with the Cr(III) product. (**B**) *Equilibrium* (i.e., steady-state) model with a constant exchange between the unreacted Cr(VI) and produced Cr(III). *Solid blue lines/curves* = the evolving δ^{53}Cr signature of the remaining (i.e., unreacted) Cr(VI) reservoir in the system. *Dashed blue lines/curves* = the δ^{53}Cr signature of an instantaneous Cr(III) product, from the reduction of Cr(VI) to Cr(III). *Redox Trajectories:* 1–2 = Partial reduction of Cr(VI) to Cr(III); 2–3 = Production of Cr(III) with an associated isotope fractionation (ε) of -0.80‰ for the reduction of Cr in marine settings (cf., Paulukat et al., 2016; Scheiderich et al., 2015). 3–4 = Incorporation of chromium (either as Cr(III), or as re-oxidized Cr(VI) species) from calcifying fluids into CaCO$_3$ biominerals. The initial Cr isotope composition used in our calculations (for local LEI seawater) has the δ^{53}Cr value ≈ 0.82‰ (i.e., a solid black circle labeled '1'). Green crosses (X) represent the δ^{53}Cr values measured in molluscan shells and microbial carbonates collected from LEI (see also data in Table 2), a black cross illustrates a specific molluscan sample LEI 05 with δ^{53}Cr of ∼0.61‰, that is modeled here considering the above *redox trajectories*. Note that a red cross with the highest δ^{53}Cr represents a sample of microbial carbonate produced by red coralline algae (LEI 10) that yielded δ^{53}Cr and Ce/Ce* which are identical with values found in local LEI seawater, suggesting a direct incorporation of Cr(VI) from seawater into CaCO$_3$ without additional biological/redox isotope fractionation.

Mg calcite) produced by calcifying red coralline algae (*Lithothamnion* sp.). This organism thus seems to incorporate Cr isotopes and REE from seawater without additional biological discrimination and/or redox-controlled isotope fractionation during biocalcification. Hence, microbial carbonates produced by certain species of calcifying algae, and their fossil counterparts (i.e., algal microbialites), could perhaps also be used as unique natural archives to trace the paleo-seawater δ^{53}Cr signature over geological time.

5.4. Plausible mechanism(s) for Cr isotope fractionation in biogenic carbonates

Pioneering studies by Wang et al. (2016) and Pereira et al. (2015) that investigated the Cr isotope fractionation between recent marine biogenic carbonates (e.g., corals, foraminifera, algae) and ambient seawater revealed that the above organisms preferentially incorporate lighter Cr isotopes into their CaCO$_3$ skeletons. These studies proposed that such enrichments in light Cr isotopes in present-day biogenic carbonates could be due to (i) the incorporation of organically complexed and particle-reactive Cr(III) species directly from seawater into CaCO$_3$, and/or (ii) via biologically-mediated redox cycling involving an initial *reduction* of marine Cr(VI) to isotopically light Cr(III), and its subsequent *re-oxidation* and incorporation into a shell. The following section models the latter scenario quantitatively, i.e., the *reduction/re-oxidation* pathway, and discusses plausible mechanisms for the observed coupling between redox-sensitive δ^{53}Cr and Ce/Ce* tracers documented in the studied molluscan shells from LEI (Fig. 5B).

5.4.1. Rayleigh Cr-isotope fractionation model for redox-controlled biocalcification

Assuming that Cr is incorporated into CaCO$_3$ minerals primarily as oxidized Cr(VI) ions (i.e., chromate CrO$_4^{2-}$ oxyanions replacing carbonate CO$_3^{2-}$ anions; Tang et al., 2007; Pereira et al., 2015), then the entire variability of a purported redox-controlled correlation between δ^{53}Cr and Ce/Ce* data in LEI molluscan shells (and/or Bahamas microbial ooids, Fig. 5B) could be explained via a partial reduction of marine Cr(VI) to Cr(III) by the organism, followed by biologically mediated re-oxidation of isotopically light Cr(III) to Cr(VI), and its eventual incorporation into CaCO$_3$ biominerals (cf., Pereira et al., 2015). The latter redox pathway (i.e.,

reduction and re-oxidation), and its effects on the δ^{53}Cr proxy, can be described quantitatively via a Rayleigh fractionation model that simulates a progressive reduction of marine Cr(VI) to Cr(III) and the associated isotope fractionation effects. Here we consider two scenarios, i.e., a *Rayleigh* and *equilibrium* fractionation models (see below, Eqs. (5) and (6)), and our calculations are based on the Cr isotope composition of a local LEI seawater (δ^{53}Cr $\approx$ 0.82‰) and a common fractionation factor (ε) of -0.80‰ for the reduction of Cr in marine settings (Paulukat et al., 2016; Scheiderich et al., 2015). Using this model parameterization, the associated changes in δ^{53}Cr of a calcifying fluid, and by inference of the precipitated biogenic carbonates (i.e., molluscan shells), can be calculated.

For the closed system *Rayleigh* fractionation (Fig. 6A) with a finite reservoir of Cr(VI) in the calcifying pool, and no exchange between the reactant Cr(VI) and produced Cr(III) species, the evolving δ^{53}Cr of a calcifying fluid (due to biologically-mediated Cr reduction) is modeled using the following equation (Ellis et al., 2002):

$$\delta^{53}\text{Cr}_{(VI)} = \left[\left(\delta^{53}\text{Cr}_{INI} + 10^3 \right) f^{(\alpha-1)} \right] - 10^3 \qquad (4)$$

where δ^{53}Cr$_{INI}$ refers to the *initial* isotope composition of an unreacted Cr(VI) pool in seawater or a calcifying fluid; f is the fraction of Cr(VI) remaining in the pool; and α is the fractionation coefficient for the biologically-mediated reduction of Cr(VI) to Cr(III), where the latter relates to the fractionation factor (ε) according to $\varepsilon \approx 1000 * \ln\alpha$.

5.4.2. Equilibrium Cr-isotope fractionation model for redox-controlled biocalcification

An alternative *equilibrium* model considers steady-state conditions where Cr(VI) and Cr(III) species interact (Fig. 6B), and here the δ^{53}Cr of a remaining Cr(VI) reactant in calcifying fluid is calculated based on (Frings et al., 2016):

$$\delta^{53}\text{Cr}_{(VI)} = \varepsilon * (1 - f) \qquad (5)$$

and an instantaneous reduced Cr(III) product being:

$$\delta^{53}\text{Cr}_{(III)} \delta^{53}\text{Cr}_{INI} + \varepsilon * f \qquad (6)$$
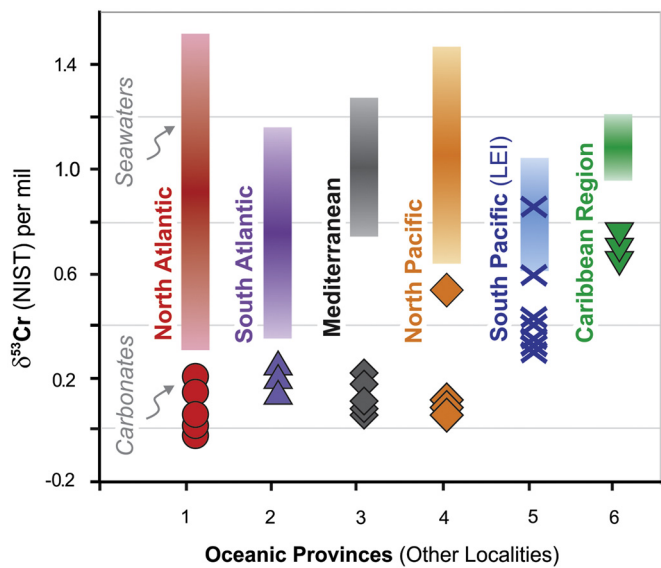
Fig. 7. A compilation of δ^{53}Cr values from recent marine biogenic carbonates (color-coded symbols) and ambient seawater (vertical colored rectangles), collected from the following oceanic provinces: South Pacific (this study), North Pacific, South and North Atlantic, Caribbean and Mediterranean Seas (seawater data from Paulukat et al., 2016; Scheiderich et al., 2015; Holmden et al., 2016; and δ^{53}Cr data from biogenic carbonates are from this study (see also Table 3), and from Bonnand et al., 2013).

In the context of the proposed *reduction* and *re-oxidation* pathway for Cr incorporation into biogenic carbonates, the above equations (Eqs. (5) and (6)) describe the first step involving the biologically-mediated *partial reduction* of marine Cr(VI) to Cr(III) at calcification sites (see also 'redox trajectories' 1–2 and 2–3 in Fig. 6). The second step (i.e., a trajectory 3–4) will then involve either (i) a direct incorporation of the produced and isotopically light Cr(III) into carbonate, or (ii) a quantitative and near complete *re-oxidation* of such light Cr(III) to Cr(VI) and its subsequent incorporation as isotopically light Cr(VI)-oxyanions into CaCO$_3$ (cf., Pereira et al., 2015; Wang et al., 2016). The latter scenario, i.e., the *re-oxidation* step (via Mn(IV) and/or microbially mediated) is however more likely, considering that under alkaline and high pH conditions typical for calcification sites, the more stable and dominant form of chromium in a solution is Cr(VI) (Pereira et al., 2015). Hence, as illustrated by 'redox trajectories' in Fig. 6, one can explain the entire variability in δ^{53}Cr and Ce/Ce* data of LEI molluscan shells via the above two-step *reduction/re-oxidation* pathway.

5.5. Chromium isotope fractionation between biogenic carbonate and seawater – a 'global ocean' perspective

To evaluate the systematics of Cr isotope fractionation between marine biogenic carbonates and ocean water on a global scale, we present a compilation of δ^{53}Cr datasets that include (i) our data from LEI and (ii) recent bivalves and gastropods from numerous locations worldwide (i.e., other locations (OL), Tables 2 and 3), which are complemented by (iii) published δ^{53}Cr data from seawaters representing the main oceanic water bodies/provinces including: North and South Atlantic, North and South Pacific Oceans, Caribbean and Mediterranean Seas (Paulukat et al., 2016; Scheiderich et al., 2015; Holmden et al., 2016). As shown in Fig. 7, marine biogenic carbonates tend to be systematically enriched in light Cr isotopes relative to local ocean waters. However, some of these shifts to lower δ^{53}Cr (i.e., those observed in OL carbonates) could also be due to the afore-mentioned contamination issues linked to a presence of lithogenic Cr, the latter causing

an early diagenetic overprint of the primary marine δ^{53}Cr signal. Nevertheless, the observed pattern of biologically controlled Cr isotope fractionation in marine carbonates is likely a common phenomenon, as it is confirmed for all our studied sites and oceanic provinces, including also our uncontaminated samples from LEI. All these sample sets showed generally lower δ^{53}Cr in marine skeletal carbonates relative to local ocean waters (Fig. 7).

5.6. Implications for δ^{53}Cr based paleo-seawater reconstructions

Due to the complex nature of Cr isotope fractionation in the seawater-carbonate system, which is controlled by both biological/kinetic and redox processes, it is challenging to interpret the Cr isotope compositions of fossil carbonates in terms of a paleo-seawater δ^{53}Cr signature. Here we use a combination of δ^{53}Cr and Ce/Ce* proxies to resolve some of these issues, as the latter can be used as an independent *redox* indicator with the aim of separating (i) the redox-controlled Cr isotope effects from (ii) a local seawater Cr isotope signal. Our results from LEI suggest that the δ^{53}Cr of paleo-seawater can be inferred from the intercept of the Ce/Ce* vs. δ^{53}Cr correlation trend for a set of well-preserved marine carbonates (e.g., molluscan shells) collected at a specific site. A similar correlation trend between δ^{53}Cr and Ce/Ce* data was also observed recently for modern ooids from Bahamas (Bonnand et al., 2013) and the intercept of this correlation also agrees with the average δ^{53}Cr of Caribbean seawater (Holmden et al., 2016).

6. Conclusions

This study investigated the chromium isotope composition (δ^{53}Cr) in present-day biogenic carbonates and seawaters collected from the southern Great Barrier Reef – Lady Elliot Island, LEI, Australia. These data from the South Pacific region are complemented by Cr isotope analysis of recent skeletal carbonates originating from the North Pacific, North and South Atlantic Oceans, Caribbean and Mediterranean Seas. Overall, the results from these globally distributed marine biogenic carbonates and local ocean waters (i.e., our and published seawater data) reveal a preferential incorporation of light Cr isotopes into marine biogenic/skeletal carbonates. However, secondary processes such as early diagenetic contamination of shells by detrital and/or lithogenic Cr phases – likely linked to Mn availability in a sediment-pore water system – can additionally shift the δ^{53}Cr of marine skeletal carbonates to lower values (i.e., approaching $-0.1‰$).

Results from LEI biogenic carbonates, with no detectable evidence for contamination, confirms the complex nature of biologically controlled incorporation of Cr into marine skeletal carbonates, which seems to be specific for different groups of calcifying organisms. In particular, molluscan shells (gastropods) showed a strong and statistically significant negative correlation between δ^{53}Cr and Ce/Ce* data ($r^2 = 0.83$, $p = 0.01$). The latter can be explained by considering (i) a partial *reduction* of isotopically heavy marine Cr(VI) to Cr(III) at calcification sites, (ii) a subsequent *re-oxidation* of isotopically light Cr(III) to Cr(VI), and (iii) its final incorporation into a shell as Cr(VI)-oxyanions replacing carbonate CO$_3^{2-}$ anions. In contrast, corals show no obvious systematic relationship with respect to local seawater Ce/Ce* and δ^{53}Cr values, but their Cr isotope composition tends to be generally lower and highly fractionated with respect to LEI ocean water. Interestingly, the only calcifying organism from LEI that yielded identical δ^{53}Cr and Ce/Ce* to those in local seawater was a microbial carbonate (i.e., high-Mg calcite) produced by calcifying red algae (*Lithothamnion* sp.).

To conclude, different carbonate producing organisms can be used in different ways to infer the Cr isotope signature of local

seawater. Our results suggest that the latter can be constrained either from (i) an intercept of Ce/Ce* vs. δ^{53}Cr correlation acquired from well-preserved molluscan shells (i.e., gastropods) and possibly ooids, or alternatively (ii) the δ^{53}Cr of local seawater can also be recorded directly by microbial carbonates produced by certain species of calcifying algae (*Lithothamnion* sp.), as the latter seems to incorporate Cr isotopes without additional biological fractionation. If validated by future studies from other locations, the above multi-proxy approach could be used to reconstruct the Cr isotope signature of paleo-seawater based on δ^{53}Cr and Ce/Ce* data in a set of well-preserved fossil marine carbonates (molluscan shells, microbialites, and possibly ooids) collected at a specific site.

Acknowledgements

Appendix A. Supplementary material

Supplementary material related to this article can be found online at https://doi.org/10.1016/j.epsl.2018.06.032.

References

Bau, M., Dulski, P., 1996. Distribution of yttrium and rare-earth elements in the Penge and Kuruman iron-formations, Transvaal Supergroup, South Africa. Precambrian Res. 79, 37–55.

Bonnand, P., James, R.H., Parkinson, I.J., Connelly, D.P., Fairchild, I.J., 2013. The chromium isotopic composition of seawater and marine carbonates. Earth Planet. Sci. Lett. 382, 10–20.

Bonnand, P., Williams, H.M., Parkinson, I.J., Wood, B.J., Halliday, A.N., 2016. Stable chromium isotopic composition of meteorites and metal–silicate experiments: implications for fractionation during core formation. Earth Planet. Sci. Lett. 435, 14–21.

Chivas, A., Chappell, J., Polach, H., Pillans, B., Flood, P., 1986. Radiocarbon evidence for the timing and rate of island development, beach-rock formation and phosphatisation at Lady Elliot Island, Queensland, Australia. Mar. Geol. 69, 273–287.

Crowe, S.A., Døssing, L.N., Beukes, N.J., Bau, M., Kruger, S.J., Frei, R., Canfield, D.E., 2013. Atmospheric oxygenation three billion years ago. Nature 501, 535–538.

D'Arcy, J., Gilleaudeau, G.J., Peralta, S., Gaucher, C., Frei, R., 2016. Redox fluctuations in the Early Ordovician oceans: an insight from chromium stable isotopes. Chem. Geol. 448, 1–12.

Daulton, T.L., Little, B.J., 2006. Determination of chromium valence over range Cr(0)–Cr(VI) by electron energy loss spectroscopy. Ultramicroscopy 106, 561–573.

de Baar, H.J.W., Bacon, M.P., Brewer, P.G., Bruland, K.W., 1985. Rare earth elements in the Pacific and Atlantic Oceans. Geochim. Cosmochim. Acta 49, 1943–1959.

De'ath, G., Fabricius, K.E., Sweatman, H., Puotinen, M., 2012. The 27-year decline of coral cover on the Great Barrier Reef and its causes. Proc. Natl. Acad. Sci. USA 109, 17995–17999.

Døssing, L.N., Dideriksen, K., Stipp, S.L.S., Frei, R., 2011. Reduction of hexavalent chromium by ferrous iron: a process of chromium isotope fractionation and its relevance to natural environments. Chem. Geol. 285, 157–166.

Elderfield, H., 1970. Chromium speciation in sea-water. Earth Planet. Sci. Lett. 9, 10–16.

Elderfield, H., 1988. The oceanic chemistry of the rare earth elements. Philos. Trans. R. Soc. Lond., Ser. A 325, 105–126.

Ellis, A.S., Johnson, T.M., Bullen, T.D., 2002. Chromium isotopes and the fate of hexavalent chromium in the environment. Science 295, 2060–2062.

Farkaš, J., Chrastný, V., Novák, M., Čadkova, E., Pašava, J., Chakrabati, R., Jacobsen, S.B., Ackerman, L., Bullen, T.D., 2013. Chromium isotope variations ($\delta^{53/52}$Cr) in mantle-derived sources and their weathering products: implications for environmental studies and the evolution of $\delta^{53/52}$Cr in the Earth's mantle over geologic time. Geochim. Cosmochim. Acta 123, 74–94.

Frei, R., Gaucher, C., Døssing, L.N., Sial, A.N., 2011. Chromium isotopes in carbonates – a tracer for climate change and for reconstructing the redox state of ancient seawater. Earth Planet. Sci. Lett. 312, 114–125.

Frei, R., Gaucher, C., Poulton, S.W., Canfield, D.E., 2009. Fluctuations in Precambrian atmospheric oxygenation recorded by chromium isotopes. Nature 461, 250–253.

Frei, R., Gaucher, C., Stolper, D., Canfield, D.E., 2013. Fluctuations in late Neoproterozoic atmospheric oxidation – Cr isotope chemostratigraphy and iron speciation of the late Ediacaran lower Arroyo del Soldado Group (Uruguay). Gondwana Res. 23, 797–811.

Frei, R., Crowe, S.A., Bau, M., Polat, A., Fowle, D.A., Døssing, L.N., 2016. Oxidative elemental cycling under low O_2 Eoarchean atmosphere. Nature, 21058. https://doi.org/10.1038/srep21058. Scientific Reports.

Frings, P.J., Clymans, W., Fontorbe, G., Christina, L., Conley, D.J., 2016. The continental Si cycle and its impact on the ocean Si isotope budget. Chem. Geol. 425, 12–36.

German, C.R., Elderfield, H., 1990. Application of the Ce anomaly as a paleoredox indicator: the ground rules. Paleoceanography 5, 823–833.

Gilleaudeau, G.J., Frei, R., Kaufman, A.J., Kah, L.C., Azmy, K., Bartley, J.K., Chernyavskiy, P., Knoll, A.H., 2016. Oxygenation of the mid-Prtoterozoic atmosphere: clues from chromium isotopes in carbonates. Geochem. Perspect. Lett. 2, 178–187.

Hamylton, S., 2014. Will coral islands maintain their growth over the next century? A deterministic model of sediment availability at Lady Elliot Island, Great Barrier Reef. PLoS ONE 9, 1–12.

Hathorne, E.C., Haley, B., Stichel, T., Grasse, P., Zieringer, M., Frank, M., 2012. Online preconcentration ICP-MS analysis of rare earth elements in seawater. Geochem. Geophys. Geosyst. 13.

Holmden, C., Jacobsen, A.D., Sageman, B.B., Hurtgen, M.T., 2016. Response of the Cr isotope proxy to Cretaceous Ocean Anoxic Event 2 in a pelagic carbonate succession from the Western Interior Seaway. Geochim. Cosmochim. Acta 186, 277–295.

Kench, P.S., Brander, R.W., 2006. Wave processes on Coral Reef Flats: implications for reef geomorphology using Australian case studies. J. Coast. Res. 22, 209–223.

Kotaś, J., Stasicka, Z., 2000. Chromium occurrence in the environment and methods of its speciation. Environ. Pollut. 107, 263–283.

McArthur, J.M., Rio, D., Massari, F., Castradori, D., Bailey, T.R., Thirlwall, M., Houghton, S., 2006. A revised Pliocene record for marine ^{87}Sr/^{86}Sr used to date an interglacial event recorded in the Cockburn Island Formation, Antarctic Peninsula. Palaeogeogr. Palaeoclimatol. Palaeoecol. 242, 126–136.

Moffett, J.W., 1990. Microbially mediated cerium oxidation in seawater. Nature 345, 421–423.

Nutman, A.P., Bennett, V.C., Friend, C.R.L., Van Kranendonk, M.J., Chivas, A.R., 2016. Rapid emergence of life shown by discovery of 3,700-million-year-old microbial structures. Nature 537, 535–538. https://doi.org/10.1038/nature19355.

Osborne, A.H., Hathorne, E.C., Schijf, J., Plancherel, Y., Boning, P., Frank, M., 2017. The potential of sedimentary foraminiferal rare earth element patterns to trace water masses in the past. Geochem. Geophys. Geosyst. 18, 1550–1568.

Paulukat, C., Gilleaudeau, G.J., Chernyavskiy, P., Frei, R., 2016. The Cr-isotope signature of surface seawater – a global perspective. Chem. Geol. 444, 101–109.

Pereira, N.S., Voegelin, A.R., Paulukat, C., Sial, A.N., Ferreira, V.P., Frei, R., 2015. Chromium-isotope signatures in scleractinian corals from the Rocas Atoll, Tropical South Atlantic. Geobiology 14, 54–67.

Pettine, M., Millero, F.J., 1990. Chromium speciation in seawater: the probable role of hydrogen peroxide. Limnol. Oceanogr. 35, 730–736.

Planavsky, N.J., Reinhard, C.T., Wang, X., Thomson, D., McGoldrick, P., Rainbird, R.H., Johnson, T., Fischer, W.W., Lyons, T.W., 2014. Low mid-Proterozoic atmospheric oxygen levels and the delayed rise of animals. Science 346, 635–638.

Rodler, A., Sanchez-Pastor, N., Fernandez-Diaz, L., Frei, R., 2015. Fractionation behavior of chromium isotopes during coprecipitation with calcium carbonate: implications for their use as paleoclimatic proxy. Geochim. Cosmochim. Acta 164, 221–235.

Rodler, A.S., Frei, R., Gaucher, C., Germs, G.J.B., 2016. Chromium isotope, REE and redox-sensitive trace element chemostratigraphy across the late Neoproterozoic Ghaub glaciation, Otavi Group, Namibia. Precambrian Res. 286, 234–249.

Scheiderich, K., Amini, M., Holmden, C., Roger, F., 2015. Global variability of chromium isotopes in seawater demonstrated by Pacific, Atlantic, and Arctic Ocean samples. Earth Planet. Sci. Lett. 423, 87–97.

Schoenberg, R., Merdian, A., Holmden, C., Kleinhanns, I.C., Haßler, K., Wille, M., Reitter, E., 2016. The stable Cr isotopic composition of chondrites and silicate planetary reservoirs. Geochim. Cosmochim. Acta 183, 14–30.

Schoenberg, R., Zink, S., Staubwasser, M., von Blanckenburg, F., 2008. The stable Cr isotope inventory of solid Earth reservoirs determined by double spike MC-ICP-MS. Chem. Geol. 249, 294–306.

Semeniuk, K., Maldonado, M.T., Jaccard, S.L., 2016. Chromium uptake and adsorption in cultured marine phytoplankton – implications for the marine Cr cycle. Geochim. Cosmochim. Acta 184, 41–54.

Shields, G., Veizer, J., 2002. Precambrian marine carbonate isotope database: version 1.1. Geochem. Geophys. Geosyst. 3, 1–12. https://doi.org/10.1029/2001GC000266. 2002.

Smith, S.V., Kroopnick, P., 1981. Carbon-13 isotopic fractionation as a measure of aquatic metabolism. Nature 294, 252–253.

Tang, Y., Elzinga, E.J., Lee, Y.J., Reeder, R.J., 2007. Coprecipitation of chromate with calcite: batch experiment and X-ray absorption spectroscopy. Geochim. Cosmochim. Acta 71, 1480–1493.

Taylor, S.R., McClennan, S.M., 1985. The Continental Crust: Its Composition and Evolution, p. 312.

Van Zuilen, M., Schoenberg, R., 2013. Cr isotopes in near surface chemical sediments. In: Melezhik, et al. (Eds.), Reading the Archive of Eart's Oxygenation, Vol. 3: Global Events and the Fennoscandian Arctic Russia – Drilling Early Earth Project. Springer-Verlag, Berlin.

Wang, X.L., Planavsky, N.J., Hull, P.M., Tripati, A.E., Zou, H.J., Elder, L., Henehan, 2016. Chromium isotopic composition of core-top planktonic foraminifera. Geobiology 14, 1–14.

Webb, G.E., Kamber, B.S., 2000. Rare earth elements in Holocene reefal microbialites: a new shallow seawater proxy. Geochim. Cosmochim. Acta 64, 1557–1565.

Wyndham, T., McCulloch, M., Fallon, S., Alibert, Ch., 2004. High-resolution coral records of rare earth elements in coastal seawater: biogeochemical cycling and new environmental proxy. Geochim. Cosmochim. Acta 68, 2067–2080.

Zaky, A.H., Brand, U., Azmy, K., 2015. A new sample processing protocol for procuring seawater REE signatures in biogenic and abiogenic carbonates. Chem. Geol. 416, 36–50.

Zink, S., Schoenberg, R., Staubwasser, M., 2010. Isotopic fractionation and reaction kinetics between Cr(III) and Cr(VI) in aqueous media. Geochim. Cosmochim. Acta 74, 5729–5745.

XMLVIEW: extended

Appendix A. Supplementary material

The following is the Supplementary material related to this article.

begin ecomponent begin ecomponent begin ecomponent begin ecomponent begin ecomponent begin ecomponent begin ecomponent begin ecomponent begin ecomponent begin ecomponent begin ecomponent begin ecomponent begin ecomponent begin ecomponent begin ecomponent begin ecomponent

`Label`: Supplementary tables and figures

`caption`: Color photographs of studied biogenic carbonates, and their taxonomic classification and mineralogy. A detailed description of analytical techniques used for mineralogical (XRD), elemental (ICP EOS, seaFAST ICP MS), and isotope analyses (TIMS) of carbonates and seawater. Complete tabulated data sets displaying elemental (Mg, Sr, Al, Mn, Fe, Cr and REE) and isotope (δ^{53}Cr, ^{87}Sr/^{86}Sr) variations measured in studied biogenic carbonates and seawater samples.

`link`: **APPLICATION : mmc1**

end ecomponent end ecomponent end ecomponent end ecomponent end ecomponent end ecomponent end ecomponent end ecomponent end ecomponent end ecomponent end ecomponent end ecomponent end ecomponent end ecomponent end ecomponent end ecomponent end ecomponent

Sponsor names

Do not correct this page. Please mark corrections to sponsor names and grant numbers in the main text.

GACR, *country*=Czechia, *grants*=15-13310S

University of Adelaide, *country*=Australia, *grants*=

ARC, *country*=Australia, *grants*=LP160101353

Danish Agency for Science, Technology and Innovation, *country*=Denmark, *grants*=11-103378, 4181-00002B

Highlights

- Cr isotopes in a seawater-carbonate system from the Great Barrier Reef, Australia.
- Systematically lower δ^{53}Cr in marine biogenic carbonates relative to ocean waters.
- Coupling between δ^{53}Cr and Ce/Ce* data in carbonates from Lady Elliot Island.
- Evidence for redox-controlled incorporation of Cr into marine biogenic carbonates.
- Implications for paleo-seawater δ^{53}Cr reconstruction based on multi-proxy approach.